

Fast and Inverse-Free Algorithms for Deflating Subspaces

James Demmel*

Ioana Dumitriu[†]Ryan Schneider*[‡]

Abstract

This paper explores a key question in numerical linear algebra: how can we compute projectors onto the deflating subspaces of a regular matrix pencil (A, B) , in particular without using matrix inversion or defaulting to an expensive Schur decomposition? We focus specifically on *spectral* projectors, whose associated deflating subspaces correspond to sets of eigenvalues/eigenvectors. In this work, we present a high-level approach to computing these projectors, which combines rational function approximation with an inverse-free arithmetic of Benner and Byers [Numerische Mathematik 2006]. The result is a numerical framework that captures existing inverse-free methods, generates an array of new options, and provides straightforward tools for pursuing efficiency on structured problems (e.g., definite pencils). To exhibit the efficacy of this framework, we consider a handful of methods in detail, including Implicit Repeated Squaring and iterations based on the matrix sign function. For the former, we present a new and general floating-point stability bound that may be of independent interest. In an appendix, we demonstrate that recent, randomized divide-and-conquer eigensolvers – which are built on fast methods for individual projectors like those considered here – can be adapted to produce the generalized Schur form of any matrix pencil in nearly matrix multiplication time.

Keywords: Matrix pencil, spectral projectors, deflating subspaces, repeated squaring, matrix sign function, generalized Schur decomposition

MSC Class: 65F15 65F60

1 Introduction

In this paper, we consider the task of computing projectors onto the right/left deflating subspaces of an arbitrary, regular matrix pencil $(A, B) \in \mathbb{C}^{n \times n} \times \mathbb{C}^{n \times n}$. We follow the standard definition for these subspaces: $\mathcal{X}, \mathcal{Y} \subseteq \mathbb{C}^n$ are right and left deflating subspaces of (A, B) , respectively, if $\dim(\mathcal{X}) = \dim(\mathcal{Y})$ and

$$\text{span}\{Ax, Bx : x \in \mathcal{X}\} = \mathcal{Y}. \quad (1.1)$$

When \mathcal{X} is spanned by a set of right eigenvectors of (A, B) , projectors onto \mathcal{X} and \mathcal{Y} are called *spectral projectors* of (A, B) .¹ If additionally $B = I$, or more generally if A and B commute, then these projectors are the same, corresponding to a single invariant eigenspace of A . Note that deflating subspaces are only defined if (A, B) is regular, which here means that the characteristic polynomial $p(\lambda) = \det(A - \lambda B)$ is *not* identically zero.

We assume throughout this section familiarity with standard definitions from linear algebra. For a summary of the relevant notation, see [Section 1.4](#).

1.1 Motivation

Spectral projectors and their associated deflating subspaces are essential in numerical linear algebra. While specific projectors/subspaces are of interest in certain applications – e.g., corresponding to the largest or

*Department of Mathematics, University of California Berkeley

[†]Department of Mathematics, University of California San Diego

[‡]Corresponding author (ryan.schneider@berkeley.edu)

¹Any set of right eigenvectors is guaranteed to span a corresponding right deflating subspace, which is easy to see from the generalized Schur form of (A, B) [39]. Despite the similarity in naming, left deflating subspaces of (A, B) are not usually spanned by left eigenvectors.

$$\begin{array}{c}
 (A, B) \\
 \longleftarrow \hspace{1.5cm} \hspace{1.5cm} \longrightarrow \\
 ((U_L^{(1)})^H A U_R^{(1)}, (U_L^{(1)})^H B U_R^{(1)}) \quad ((U_L^{(2)})^H A U_R^{(2)}, (U_L^{(2)})^H B U_R^{(2)})
 \end{array}$$

Figure 1: One step of divide-and-conquer applied to the pencil (A, B) , where $U_R^{(1)}, U_L^{(1)}$ and $U_R^{(2)}, U_L^{(2)}$ are rectangular matrices containing bases for pairs of deflating subspaces.

smallest k eigenvalues as in [38] – our primary motivation is a specific subproblem of divide-and-conquer eigensolvers, which recursively diagonalize a matrix pencil (or individual matrix, setting $B = I$) as in Figure 1.

Here, $U_R^{(1)}, U_L^{(1)} \in \mathbb{C}^{n \times k}$ and $U_R^{(2)}, U_L^{(2)} \in \mathbb{C}^{n \times (n-k)}$ contain orthonormal bases for pairs of right/left deflating subspaces corresponding to disjoint sets of eigenvalues. Typically, these matrices are obtained by first computing the associated projectors and subsequently rank-revealing factorizations for them. In this way, the projectors are the key ingredient of divide-and-conquer; because they are linked to deflating subspaces spanned by eigenvectors, it is not difficult to show that the spectra of the $k \times k$ and $(n-k) \times (n-k)$ subproblems form a disjoint union of the spectrum of (A, B) .

While divide-and-conquer has existed in the literature for several decades [2, 3, 7, 10, 29], it has only recently been formulated in a way that provably succeeds (and achieves near-optimal complexity) on arbitrary inputs [6, 14]. As efforts to deploy these algorithms move forward, optimizing methods for computing projectors is increasingly important, as the step of divide-and-conquer that relies on them tends to dominate in both computational time and precision requirements. With this in mind, we focus specifically on the following problem, which – as is typical in divide-and-conquer – assumes that we have already identified a region of the complex plane containing a piece of the spectrum of (A, B) .

Problem Statement. Given an arbitrary, regular matrix pencil (A, B) and a set $S \subseteq \mathbb{C}$ containing some subset of eigenvalues of (A, B) , compute the projectors P_R and P_L onto the right/left deflating subspaces corresponding to S , where the former is spanned by the (right) eigenvectors associated to eigenvalues in S and the latter is defined according to (1.1).

Our primary contribution in this paper is a general framework for developing fast, inverse-free algorithms that can solve this problem. Here, “fast” means that each method requires at most $O(\log(\frac{n}{\delta})T_{\text{MM}}(n))$ operations to compute P_R and P_L to forward accuracy δ in the spectral norm – assuming the problem is not too ill-conditioned – for $T_{\text{MM}}(n)$ the complexity of $n \times n$ matrix multiplication. Several such algorithms already exist in the literature (and are summarized in the subsequent sections); our framework provides a means of understanding/adapting them and generating new options.

Conditioning in this setting depends primarily on the largest $\epsilon > 0$ for which the ϵ -pseudospectrum of (A, B) , defined appropriately (see Definition 3.11), is well-separated from the boundary of S . To achieve the “fast” moniker this ϵ will need to be at least polynomial in n^{-1} and δ , as we discuss further in Section 3. Note that this notion of ill-conditioning speaks to complexity and not feasibility/accuracy; the methods we present can still produce accurate approximations even if the pseudospectral condition does not hold, though in that case they exceed $O(\log(\frac{n}{\delta})T_{\text{MM}}(n))$ complexity. A problem is ill-posed only when (A, B) has an eigenvalue on the boundary of S .

Remark 1.1. Absent these fast methods, computing P_R and P_L typically requires obtaining a full Schur decomposition of (A, B) and reorganizing it so that the leading eigenvalues belong to S – i.e., `xGGES` in LAPACK.² Indeed, computing a generalized Schur decomposition is equivalent to computing a sequence of nested deflating subspaces. With this in mind, and because Schur form itself has a variety of applications [1, 15, 16, 18], we discuss it in more detail in Appendix A. There we demonstrate that the aforementioned divide-and-conquer approach can be adapted to produce a Schur decomposition (of any pencil in nearly matrix multiplication time) by leveraging the fast methods for individual deflating subspaces presented in the rest of the paper.

²See [24] for a discussion of the reorganization procedure.

1.2 High-Level Strategy

At a high level, our goal will be to transform (A, B) into the pencil (A_S, B_S) , which has the same right eigenvectors as (A, B) but whose eigenvalues are zero and one, depending on whether or not the corresponding eigenvalues of (A, B) belong to S . If this can be done, obtaining projectors is straightforward; in particular, $P_R = B_S^{-1}A_S$. Moreover, P_L^H can be obtained by repeating this procedure with (A^H, B^H) and $S^* = \{\bar{z} : z \in S\}$.³ Since a rank-revealing QR factorization of $B_S^{-1}A_S$ can be computed implicitly, for example using the **GRURV** algorithm of Ballard et al. [4], accomplishing the transformation $(A, B) \rightarrow (A_S, B_S)$ is sufficient for computing P_R and P_L without inversion.

In practice, obtaining (A_S, B_S) from (A, B) naturally reduces to (rationally) approximating the indicator function

$$\mathbb{1}_S(z) = \begin{cases} 1 & z \in S \\ 0 & z \in \mathbb{C} \setminus \bar{S} \\ \text{undefined} & z \in \partial S \end{cases} \quad (1.2)$$

where \bar{S} denotes the closure of S . Evaluating such an approximation $r(z)$ at $B^{-1}A$ (without taking inverses or forming the product) will yield an approximation of (A_S, B_S) , as doing so preserves right eigenvectors while mapping eigenvalues λ to $r(\lambda)$. Work of Benner and Byers [8, 9], which develops an inverse-free arithmetic on matrix pencils, implies that this can be done implicitly. The central definition of their arithmetic is the *matrix relation*

$$(B \setminus A) = \{(x, y) \in \mathbb{C}^n \times \mathbb{C}^n : Ax = By\}, \quad (1.3)$$

which we can think of as a representation⁴ of $B^{-1}A$ that neither requires B to be invertible nor risks instability if B is invertible but ill-conditioned. The corresponding arithmetic is defined by the following operations.

Definition 1.2 (Arithmetic for Matrix Relations). The *sum* and *product* of two matrix relations $(B_1 \setminus A_1)$ and $(B_2 \setminus A_2)$ are subsets of $\mathbb{C}^n \times \mathbb{C}^n$ given by

$$(B_2 \setminus A_2) + (B_1 \setminus A_1) = \left\{ (x, z) : \exists y_1, y_2 \text{ s.t. } \begin{pmatrix} A_1 & -B_1 & 0 & 0 \\ A_2 & 0 & -B_2 & 0 \\ 0 & I & I & -I \end{pmatrix} \begin{pmatrix} x \\ y_1 \\ y_2 \\ z \end{pmatrix} = 0 \right\}$$

$$(B_2 \setminus A_2)(B_1 \setminus A_1) = \left\{ (x, z) : \exists y \text{ s.t. } \begin{pmatrix} A_1 & -B_1 & 0 \\ 0 & A_2 & -B_2 \end{pmatrix} \begin{pmatrix} x \\ y \\ z \end{pmatrix} = 0 \right\}.$$

Observing that a block QR factorization

$$\begin{pmatrix} A \\ B \end{pmatrix} = \begin{pmatrix} Q_{11} & Q_{12} \\ Q_{21} & Q_{22} \end{pmatrix} \begin{pmatrix} R \\ 0 \end{pmatrix} \quad (1.4)$$

implies $\text{null}([Q_{12}^H \ Q_{22}^H]) = \text{range}\left(\begin{bmatrix} A \\ B \end{bmatrix}\right)$, another result of Benner and Byers suggests that the sum and product of any pair of matrix relations can be computed using only QR and matrix multiplication [9, Theorems 2.3 and 2.7].

Theorem 1.3 (Benner and Byers 2006). *Let $(B_1 \setminus A_1)$ and $(B_2 \setminus A_2)$ be two matrix relations with $A_1, A_2, B_1, B_2 \in \mathbb{C}^{n \times n}$. Suppose*

$$\text{null}([Q_1 \ Q_2]) = \text{range}\left(\begin{bmatrix} -B_1 \\ A_2 \end{bmatrix}\right) \quad \text{and} \quad \text{null}([U_1 \ U_2]) = \text{range}\left(\begin{bmatrix} -B_1 \\ B_2 \end{bmatrix}\right).$$

³This follows from the observation that left eigenvectors of $B^{-H}A^H$ associated to S – which are not necessarily left eigenvectors of either (A, B) or (A^H, B^H) – span the appropriate left deflating subspace.

⁴This representation is not unique. We can left multiply A and B by any matrix M whose null space only trivially overlaps with the range of $\begin{bmatrix} A & B \end{bmatrix}$ without changing the relation.

Then

$$(B_2 \setminus A_2)(B_1 \setminus A_1) = ((Q_2 B_2) \setminus (Q_1 A_1))$$

and

$$(B_2 \setminus A_2) + (B_1 \setminus A_1) = ((U_2 B_2) \setminus (U_1 A_1 + U_2 A_2)).$$

It can be shown that these operations extend to the spectra of (A_1, B_1) and (A_2, B_2) in a natural way; if λ and μ are eigenvalues of these pencils associated to a shared (right) eigenvector v , then $(\lambda + \mu, v)$ and $(\lambda\mu, v)$ are eigenpairs of the pencils corresponding to $(B_2 \setminus A_2) + (B_1 \setminus A_1)$ and $(B_2 \setminus A_2)(B_1 \setminus A_1)$, respectively⁵ [9, Theorems 2.5 and 2.8]. Hence, a polynomial can be applied to a regular pencil (A, B) by evaluating it at the relation $(B \setminus A)$, which implicitly evaluates the polynomial at $B^{-1}A$ and maps eigenvalues accordingly.

To extend this to rational functions we need only introduce some notion of a multiplicative inverse, which can be done as $(B \setminus A)^{-1} = (A \setminus B)$. While this is only a true inverse when $B^{-1}A$ exists and is invertible, it is sufficient for our purposes since the eigenvalues of (B, A) are clearly the reciprocals of the eigenvalues of (A, B) , again corresponding to the same right eigenvectors.⁶

Given any rational function $r(z) = p(z)/q(z)$ for polynomials p and q , we can now evaluate $r(B \setminus A)$ using the arithmetic of Benner and Byers as

$$r(B \setminus A) = (q(B \setminus A))^{-1} p(B \setminus A). \tag{1.5}$$

Here we make a somewhat arbitrary choice; we could evaluate $r(B \setminus A)$ as $p(B \setminus A)(q(B \setminus A))^{-1}$, though this simply yields a different representation of the same matrix relation. Sticking with (1.5), we obtain the following high-level, inverse-free framework for computing (A_S, B_S) :

1. Approximate the indicator function $\mathbb{1}_S(z)$ with a rational function $r(z)$.
2. Evaluate $r(B \setminus A)$ using only matrix multiplication and QR via [Theorem 1.3](#) and (1.4).
3. Set $(B_S \setminus A_S) = r(B \setminus A)$.

In this framework, each choice of $r(z)$ generates a different numerical method for solving our original problem. To choose between them, we suggest the following.

The Indicator Approximation Problem: Given $S \subseteq \mathbb{C}$, what is the “best” rational function approximation to $\mathbb{1}_S(z)$?

This question is more subtle than it initially appears. While in general we prefer approximations that are as close to $\mathbb{1}_S(z)$ as possible – in an appropriate norm and at least near the eigenvalues of (A, B) if not on all of S – we must also account for the expensive nature of Benner and Byer’s inverse-free arithmetic. That is, each addition/multiplication required to evaluate a given rational function requires a block $2n \times n$ QR factorization. Hence, a better approximation to $\mathbb{1}_S(z)$ may not yield a more efficient method if it requires even one or two additional operations. There is one exception here: Möbius transformations; $r(z) = \frac{az+b}{cz+d}$ can be applied to $(B \setminus A)$ for free as $((cA + dB) \setminus (aA + bB))$, and it will therefore be advantageous to write $r(z)$ in terms of Möbius transformations whenever possible.

In light of these observations, the Indicator Approximation Problem can be used not just to choose an approximation but to refine it, perhaps based on more specific knowledge of where eigenvalues lie in S . This is our motivation for leaving the problem open-ended; the meaning of “best” and any corresponding answer will depend on (A, B) , S , and the computational resources available. Because of this flexibility, we position the Indicator Approximation Problem as a natural tool for algorithmic optimization, and we demonstrate in the subsequent sections how it can streamline the development of more efficient methods.

Regardless of the choice of $r(z)$, the framework outlined above naturally promotes stability in floating-point arithmetic by avoiding matrix inversion. This is particularly valuable when working with a pencil (A, B) in which B and/or A is singular or nearly singular. Moreover, it leaves the door open to implement any of the methods considered here in a communication-optimal fashion (in the vein of Ballard et al. [5]). These concerns are especially relevant for divide-and-conquer eigensolvers, where the benefits of avoiding inversion have already been explored – e.g., [3, 14, 36].

⁵Technically, this only holds if (A_1, B_1) and (A_2, B_2) are both regular and $\{\lambda, \mu\} \neq \{\infty, 0\}$, though this will always be the case for our purposes.

⁶Note that if (A, B) has an eigenvalue at zero then (B, A) has a corresponding eigenvalue at infinity.

Method	S	Approximation $r(z)$
Implicit Repeated Squaring	$ z < 1$	$(1 + z^{2^k})^{-1}$
Newton Iteration	$\operatorname{Re}(z) > 0$	$f \circ \dots \circ f(z)$ with $f(z) = \frac{1}{2}(z + z^{-1})$
Halley Iteration	$\operatorname{Re}(z) > 0$	$f \circ \dots \circ f(z)$ with $f(z) = z \frac{z^2+3}{3z^2+1}$
Dynamically Weighted Halley Iteration	$\operatorname{Re}(z) > 0$	$f_k \circ \dots \circ f_1(z)$ with $f_i(z) = z \frac{a_i z^2 + b_i}{c_i z^2 + d_i}$

Table 1: Methods of approximating $\mathbb{1}_S(z)$ for different choices of S . The Newton and Halley iterations are based on the (complex) scalar sign function (3.2), as $\mathbb{1}_S(z) = \frac{1}{2}(\operatorname{sign}(z) + 1)$ if S is the right half plane.

1.3 Contributions

In the remainder of the paper, we discuss a handful of specific instances of our high-level framework, which are summarized in Table 1. Our goal throughout is to produce rigorous performance guarantees for each method. Since all four can be implemented iteratively – either by implementing the composition of a fixed rational function or via iterative squaring – relative efficiency will be determined by the operation count per iteration and the total number of iterations required to reach a given level of accuracy. As we will see, executing k iterations of each method requires $O(kT_{\text{MM}}(n))$ operations.

The main contributions of the remaining sections can now be summarized as follows:

- In Section 2, we consider the Implicit Repeated Squaring (**IRS**) routine of Malyshev [29], arguably the most widely used inverse-free method for computing projectors. We include in this section a new, general stability bound for the method in floating-point arithmetic, which is based on a standard finite-precision model that can accommodate fast matrix multiplication.
- Section 3 subsequently presents inverse-free methods based on the matrix sign function of Beavers and Denman [7]. There, we use the Indicator Approximation Problem to refine one of these methods – the Halley iteration – in an effort to improve efficiency on problems with real eigenvalues.⁷ The result is a new (generalized) dynamically weighted Halley iteration.
- In Section 4, we provide a handful of numerical examples that test the methods explored in the preceding sections.
- Finally, Appendix A presents the aforementioned discussion of divide-and-conquer for Schur form, Appendix B contains the proof of the finite-precision stability bound for **IRS**, and Appendix C covers additional numerical examples.

In total, this work demonstrates the efficacy of the previous section’s high-level framework, both as a tool to understand and adapt existing methods and to produce new ones. To that end, we hope it prompts further development of specialized routines for this problem.

1.4 Notation and Conventions

Throughout the paper, we use $(A, B) \in \mathbb{C}^{n \times n} \times \mathbb{C}^{n \times n}$ to denote a square matrix pencil, which is assumed to be regular. A^H and A^{-H} denote the Hermitian transpose and inverse Hermitian transpose, respectively, while I is used to denote the identity matrix, with size implied by context. $\|\cdot\|_2$ is the spectral norm on matrices and the Euclidean norm on vectors, and $\kappa_2(\cdot)$ is the spectral norm condition number. $\Lambda(A, B)$ is used to denote the spectrum of (A, B) . Finally, $\sigma_i(A)$ is the i -th singular value of A , though when convenient $\sigma_{\min}(A)$ may be used to denote the smallest singular value of A instead.

2 Implicit Repeated Squaring

We start with Implicit Repeated Squaring (**IRS**), a routine for repeatedly squaring a product $A^{-1}B$ without forming it. **IRS** originates in early efforts to implement inverse-free, divide-and-conquer eigensolvers, first

⁷This includes the important definite generalized eigenvalue problem. See [41, Section VI.3] for further background.

in work⁸ of Malyshev [25, 26] and later Bai, Demmel, and Gu [2]. It eventually appeared as in Algorithm 1 – with the name **IRS** – in work of Ballard, Demmel, and Dumitriu [3].

Algorithm 1 Implicit Repeated Squaring (**IRS**)

Input: $A, B \in \mathbb{C}^{n \times n}$ and p a positive integer.

```

1:  $A_0 = A$ 
2:  $B_0 = B$ 
3: for  $j = 0 : p - 1$  do
4:    $\begin{pmatrix} B_j \\ -A_j \end{pmatrix} = \begin{pmatrix} Q_{11} & Q_{12} \\ Q_{21} & Q_{22} \end{pmatrix} \begin{pmatrix} R_j \\ 0 \end{pmatrix}$ 
5:    $A_{j+1} = Q_{12}^H A_j$ 
6:    $B_{j+1} = Q_{22}^H B_j$ 
7: end for
8: return  $A_p, B_p$ 

```

IRS can be used to compute projectors by applying our framework with $r(z) = (1 + z^{2^p})^{-1}$ and $S = \{z : |z| < 1\}$. In these terms, the pseudocode of Algorithm 1 can be viewed as a straightforward application of Theorem 1.3 to $(A_p \setminus B_p) = (A \setminus B)^{2^p}$, where squaring naturally drives eigenvalues to zero and infinity (assuming none are on the unit circle). Applying the Möbius transformation $(1 + z)^{-1}$, which sends zero to one and infinity to zero, the projector P_R can be obtained from $((A_p + B_p) \setminus A_p)$ as

$$P_R \approx (A_p + B_p)^{-1} A_p. \quad (2.1)$$

Repeating this process with (A^H, B^H) yields the left projector $P_L \approx \mathcal{A}_p^H (A_p + B_p)^{-H}$ for $(A_p \setminus B_p) = (A^H \setminus B^H)^{2^p}$. Note here that **IRS** is applied to $(A \setminus B)$ rather than $(B \setminus A)$. This is done to maintain consistency with the presentation of **IRS** in [2, 3], though it also means that P_R and P_L are spectral projectors of (A, B) corresponding to $\{z : |z| > 1\}$ rather than S . To avoid confusion, we label the projectors as $P_{R,|z|>1}$ and $P_{L,|z|>1}$ to make clear the subset of the spectrum of (A, B) they depend on.

2.1 Condition Number

Exact-arithmetic accuracy bounds for **IRS** have historically been presented in terms of one of the following two quantities. First is $\omega_{(A,B)}$ – the “criterion of absence of eigenvalues of the pencil $\lambda B - A$ on the unit circle and within a small neighborhood of it” introduced⁹ by Malyshev [29]. While the formal definition of $\omega_{(A,B)}$ covers only regular pencils, it easily extends to singular pencils by setting $\omega_{(A,B)} = \infty$.

Definition 2.1. For a regular pencil (A, B)

$$\omega_{(A,B)} = \left\| \frac{1}{2} \int_0^{2\pi} (B - e^{i\phi} A)^{-1} (AA^H + BB^H) (B - e^{i\phi} A)^{-H} d\phi \right\|_2.$$

Aiming to replace $\omega_{(A,B)}$ with something more straightforward, Bai, Demmel, and Gu subsequently analyzed **IRS** in terms of a distance to the nearest ill-posed problem $d_{(A,B)}$ [2].

Definition 2.2. The distance from (A, B) to the nearest ill-posed problem is

$$d_{(A,B)} = \inf \{ \|E\|_2 + \|F\|_2 : (A + E) - z(B + F) \text{ is singular for some } |z| = 1 \}.$$

Both $\omega_{(A,B)}$ and $d_{(A,B)}$ are specialized to the setting where **IRS** is employed to compute spectral projectors. Indeed, recalling (2.1), Malyshev [29, Equation 23] and Bai, Demmel, and Gu [2, Theorem 1] bound $\|(A_p + B_p)^{-1} A_p - P_{R,|z|>1}\|_2$ in terms of $\omega_{(A,B)}$ and $d_{(A,B)}^{-1}$, respectively. Moreover, $\omega_{(A,B)}$ and $d_{(A,B)}^{-1}$ are infinite if (A, B) is singular or has an eigenvalue on the unit circle, in which case squaring cannot successfully

⁸The paper [26] was translated from Russian in two parts [27, 28]. Much of its content was subsequently presented in [29].

⁹Malyshev’s definition is a generalized and scale invariant version of a similar quantity of Bulgakov and Godunov [10].

produce a projector by driving eigenvalues to zero and infinity. As a result, both have been cast as condition numbers for the procedure.¹⁰

We seek something more general here. Our motivation lies in the potential for **IRS** to be applied to other problems in numerical linear algebra. Take for example the matrix exponential e^A . The most commonly used algorithm for computing e^A is the scaling and squaring method [23], which evaluates the exponential as

$$e^A \approx [q(A/2^p)^{-1}p(A/2^p)]^{2^p} \quad (2.2)$$

for two polynomials p and q . Clearly, **IRS** can be used to handle the squaring step of this approach without relying on inversion. Nevertheless, the aforementioned condition numbers are ill-suited to capture its performance, since eigenvalues of $(q(A/2^p), p(A/2^p))$ on the unit circle are irrelevant.

With this in mind, we choose to work with the following condition number.

Definition 2.3. Given $A, B \in \mathbb{C}^{n \times n}$ and $p \geq 1$, define the block matrix

$$D_{(A,B)}^p = \begin{pmatrix} B & & & \\ -A & B & & \\ & -A & \ddots & \\ & & \ddots & B \\ & & & -A \end{pmatrix} \in \mathbb{C}^{2^p n \times (2^p - 1)n}.$$

The *condition number* of **IRS** corresponding to the inputs A, B , and p is

$$\kappa_{\text{IRS}}(A, B, p) = \sigma_{\min}(D_{(A,B)}^p)^{-1} \left\| \begin{pmatrix} A \\ B \end{pmatrix} \right\|_2.$$

It is not hard to show that $\kappa_{\text{IRS}}(A, B, p)$ is invariant to both swapping A and B and scaling (A, B) , and it also satisfies $\kappa_{\text{IRS}}(A, B, p) \geq 1$ for any inputs.¹¹ Moreover, we have the following lemma, which suggests that bounds involving $\kappa_{\text{IRS}}(A, B, p)$ should be sharper than existing results.

Lemma 2.4. *Let (A, B) be an $n \times n$ regular pencil. Then for any $p \geq 1$ we have*

$$\sigma_{\min}(D_{(A,B)}^p) \geq d_{(A,B)} \geq \frac{\sqrt{\sigma_n(AA^H + BB^H)}}{14\omega_{(A,B)}}$$

Proof. Let $m = 2^p$ and define the $mn \times mn$ block matrix

$$M_p(A, B) = \begin{pmatrix} -A & & & -B \\ B & -A & & \\ & \ddots & \ddots & \\ & & B & -A \end{pmatrix}. \quad (2.3)$$

To first show $\sigma_{\min}(D_{(A,B)}^p) \geq \sigma_{\min}(M_p(A, B))$, let $x = [x_1 \ x_2 \ \cdots \ x_{m-1}]^T \in \mathbb{C}^{(m-1)n}$ be the unit vector satisfying $\sigma_{\min}(D_{(A,B)}^p) = \|D_{(A,B)}^p x\|_2$, where $x_i \in \mathbb{C}^n$ for each i . Padding x with zeros to obtain another unit vector

$$y = [x_{m-1} \ x_{m-2} \ \cdots \ x_1 \ 0] \in \mathbb{C}^{mn} \quad (2.4)$$

it is easy to see $\|M_p(A, B)y\|_2 = \|D_{(A,B)}^p x\|_2$ and therefore

$$\sigma_{\min}(M_p(A, B)) \leq \|M_p(A, B)y\|_2 = \|D_{(A,B)}^p x\|_2 = \sigma_{\min}(D_{(A,B)}^p). \quad (2.5)$$

¹⁰Note, however, that $d_{(A,B)}$ is not invariant to scaling since $d_{(\alpha A, \alpha B)} = |\alpha|d_{(A,B)}$. For this reason, results of Bai, Demmel, and Gu are stated in terms of $\frac{\|(A \ B)\|_2}{d_{(A,B)}}$ for $(A \ B)$ the $n \times 2n$ matrix obtained by concatenating A and B .

¹¹This follows from the observation $\sigma_{\min}(D_{(A,B)}^p) \leq \sigma_{\min}\begin{pmatrix} A \\ B \end{pmatrix}$.

The first inequality now follows from an observation of Bai, Demmel, and Gu, who show that $M_p(A, B)$ is unitarily equivalent to the block matrix $\text{diag}(-A + e^{i\theta_1}B, \dots, -A + e^{i\theta_m}B)$ for $e^{i\theta_1}, \dots, e^{i\theta_m}$ the m^{th} roots of -1 . Hence, we have

$$\sigma_{\min}(M_p(A, B)) = \min_{1 \leq j \leq m} \sigma_n(-A + e^{i\theta_j}B) \geq \min_{\theta} \sigma_n(-A + e^{i\theta}B) = d_{(A, B)}. \quad (2.6)$$

The remaining inequality can be derived from [29, Theorem 3]. Letting $LL^H = AA^H + BB^H$ be a Cholesky factorization (which exists since (A, B) is regular) and setting $A_0 = L^{-1}A$ and $B_0 = L^{-1}B$, we have

$$\frac{1}{14\omega_{(A, B)}} < \frac{1}{\max_{\phi} \|(B_0 - e^{i\phi}A_0)^{-1}\|_2} \leq \|L^{-1}\|_2 \min_{\phi} (B - e^{i\phi}A) = \frac{d_{(A, B)}}{\sigma_n(L)}. \quad (2.7)$$

We complete the proof by rearranging and recalling $\sigma_i(L)^2 = \sigma_i(AA^H + BB^H)$ for all i . \square

As we might expect, $\kappa_{\text{IRS}}(A, B, p)$ is not necessarily infinite if (A, B) has an eigenvalue on the unit circle.¹² It is also the only condition number considered here that has an explicit dependence on p , the number of steps of squaring. While $\kappa_{\text{IRS}}(A, B, p)$ increases with p , Lemma 2.4 implies the p -independent upper bound

$$\kappa_{\text{IRS}}(A, B, p) \leq d_{(A, B)}^{-1} \left\| \begin{pmatrix} A \\ B \end{pmatrix} \right\|_2. \quad (2.8)$$

Thinking of p as an input to the procedure not only provides a tighter condition number but also allows us to quantify the stability of **IRS** in terms of the number of steps taken (and its dependence on n).

2.2 Floating-Point Stability Bound

With $\kappa_{\text{IRS}}(A, B, p)$ at our disposal, we now pursue a rigorous and general stability bound for **IRS** in finite-precision arithmetic. Here, we assume a floating-point (i.e., finite-precision) model of computation, where

$$fl(x \circ y) = (x \circ y)(1 + \Delta), \quad |\Delta| \leq \mathbf{u} \quad (2.9)$$

for basic operations $\circ \in \{+, -, \times, \div\}$ and a machine precision $\mathbf{u}(\epsilon, n)$, which is a function of the desired accuracy ϵ and the size of the problem n . This is a standard formulation for finite-precision arithmetic (see for example [22]). Given \mathbf{u} , the number of bits of precision required to achieve (2.9) is $\log_2(1/\mathbf{u})$.

To analyze **IRS** in this model, we further assume access to the following black-box algorithms for QR and matrix multiplication, where $\mu_{\text{MM}}(n)$ and $\mu_{\text{QR}}(n)$ are (low-degree) polynomials in n .

Assumption 2.5 (Matrix Multiplication). There exists a $\mu_{\text{MM}}(n)$ -stable $n \times n$ multiplication algorithm $\text{MM}(\cdot, \cdot)$ satisfying

$$\|\text{MM}(A, B) - AB\|_2 \leq \mu_{\text{MM}}(n)\mathbf{u}\|A\|_2\|B\|_2$$

in $T_{\text{MM}}(n)$ arithmetic operations.

Assumption 2.6 (QR Factorization). There exists a $\mu_{\text{QR}}(n)$ -stable full QR algorithm $\text{QR}(\cdot)$ satisfying

1. $[Q, R] = \text{QR}(A)$ for $A, R \in \mathbb{C}^{2n \times n}$ and $Q \in \mathbb{C}^{2n \times 2n}$.
2. R is exactly upper triangular
3. There exist $A' \in \mathbb{C}^{2n \times n}$ and unitary $Q' \in \mathbb{C}^{2n \times 2n}$ such that $A' = Q'R$ with

$$\|Q' - Q\|_2 \leq \mu_{\text{QR}}(n)\mathbf{u} \quad \text{and} \quad \|A' - A\|_2 \leq \mu_{\text{QR}}(n)\mathbf{u}\|A\|_2,$$

in $T_{\text{QR}}(n)$ arithmetic operations.

¹²Instead, $\kappa_{\text{IRS}}(A, B, p)$ is infinite when a block QR factorization of $D_{(A, B)}^p$ cannot be controlled by standard perturbation bounds. Accordingly, it is less a measure of the extent to which a problem is ill-posed for implicit squaring and more an artifact of our analysis (see Appendix B).

Once again, these black-box assumptions are somewhat standard [22, Section 3.5 and Chapter 19]. While we won't be too particular about $\mu_{\text{MM}}(n)$ and $\mu_{\text{QR}}(n)$, we do note that they are compatible with fast¹³ matrix multiplication; that is, QR can be implemented stably (in a mixed sense) using fast matrix multiplication [12], which itself can be formulated to satisfy the forward error bound given by Assumption 2.5 [13]. Consequently our analysis applies to **IRS** implemented with a variety of fast matrix multiplication routines [11, 42, 44], including the current fastest known algorithm of Williams et al. [45], and we may additionally assume $T_{\text{QR}}(n) = O(T_{\text{MM}}(n))$.

In terms of these black-box assumptions, each iteration of **IRS** consists of the following.

1. $[Q, R] = \mathbf{QR} \left(\begin{bmatrix} B_j \\ -A_j \end{bmatrix} \right)$ with $Q = \begin{pmatrix} Q_{11} & Q_{12} \\ Q_{21} & Q_{22} \end{pmatrix}$
2. $A_{j+1} = \mathbf{MM}(Q_{12}^H, A_j)$
3. $B_{j+1} = \mathbf{MM}(Q_{22}^H, B_j)$

Allowing the error guarantees implied by our black-box assumptions to propagate through multiple iterations yields the following (weak) forward stability bound for the algorithm overall.

This is not the first time that **IRS** has been analyzed in finite-precision arithmetic. In fact, the proof of Theorem 2.7, which we defer to Appendix B, follows an argument originally developed by Malyshev [27]. We generalize this work by demonstrating that Malyshev's analysis can accommodate the rigorous floating-point assumptions summarized above (and therefore also finite-precision, fast matrix multiplication). Moreover, since Theorem 2.7 is stated in terms of $\kappa_{\text{IRS}}(A, B, p)$ it is usable in both the spectral projector setting and more general applications.

Theorem 2.7. *Given $A, B \in \mathbb{C}^{n \times n}$ and $p \geq 1$, let $[\tilde{A}_p, \tilde{B}_p] = \mathbf{IRS}(A, B, p)$ on a floating-point machine with precision \mathbf{u} . For $\epsilon \in (0, 1)$ and $\mu(n) = \max\{\mu_{\text{MM}}(n), \mu_{\text{QR}}(n), \sqrt{n}\}$ suppose*

$$\mathbf{u} \leq \frac{\epsilon}{324\mu(n)\kappa_{\text{IRS}}(A, B, p) \max\{p^2 + 4p - 5, 1\}}.$$

Then there exist matrices $\mathring{A}_p, \mathring{B}_p \in \mathbb{C}^{n \times n}$ such that $\mathring{A}_p^{-1}\mathring{B}_p = (A^{-1}B)^{2p}$ and

$$\|\tilde{A}_p - \mathring{A}_p\|_2, \|\tilde{B}_p - \mathring{B}_p\|_2 \leq \epsilon \left\| \begin{pmatrix} A \\ B \end{pmatrix} \right\|_2.$$

Theorem 2.7 implies that the number of bits of precision required for **IRS** to compute \tilde{A}_p and \tilde{B}_p to within $\epsilon \left\| \begin{pmatrix} A \\ B \end{pmatrix} \right\|_2$ of a corresponding set of exact outputs is at most

$$\log_2(1/\mathbf{u}) = O(\log_2(1/\epsilon) + \log_2(\mu(n)) + \log_2(\kappa_{\text{IRS}}(A, B, p)) + \log_2(p)). \quad (2.10)$$

When used to compute projectors as part of the randomized versions of divide-and-conquer developed in [6, 14], this precision requirement is provably lower, in general, than alternatives that require inversion (see the discussion in [36, Chapter 6]).

3 Sign Function Methods

We consider next a family of methods based around the matrix sign function. In terms of our high-level framework, S is now the right half plane, in which case

$$\mathbf{1}_S(z) = \frac{1}{2}(\text{sign}(z) + 1), \quad (3.1)$$

for $\text{sign}(z)$ the scalar sign function

$$\text{sign}(z) = \begin{cases} +1 & \text{Re}(z) > 0 \\ -1 & \text{Re}(z) < 0 \\ \text{undefined} & \text{otherwise.} \end{cases} \quad (3.2)$$

¹³i.e., sub- $O(n^3)$

Algorithm 2 Inverse-Free Newton Iteration (**IF-Newton**)**Input:** $A, B \in \mathbb{C}^{n \times n}$, p a number of iterations.**Requires:** (A, B) has no eigenvalues on $\text{Re}(z) = 0$.

```

1:  $A_0 = A$ 
2:  $B_0 = B$ 
3: for  $j = 0 : p - 1$  do
4:    $\begin{pmatrix} -A_j \\ B_j \end{pmatrix} = \begin{pmatrix} Q_{11} & Q_{12} \\ Q_{21} & Q_{22} \end{pmatrix} \begin{pmatrix} R_j \\ 0 \end{pmatrix}$ 
5:    $A_{j+1} = \frac{1}{\sqrt{2}}(Q_{12}^H B_j + Q_{22}^H A_j)$ 
6:    $B_{j+1} = \sqrt{2}Q_{22}^H B_j$ 
7: end for
8: return  $(A_p, B_p)$ 

```

In this setting, approximations of $\mathbf{1}_S(z)$ can be derived from approximations of $\text{sign}(z)$, and moreover computing P_R and P_L reduces to approximating (implicitly) the matrix sign function $\text{sign}(B^{-1}A)$, as defined by Roberts [35]. Accordingly, eigenvalues are driven to ± 1 .

3.1 Newton Iteration

The most commonly used method for approximating $\text{sign}(A)$ is a simple Newton iteration of Roberts [35]. From the viewpoint of function approximation, this iteration computes $\text{sign}(z)$ via the rational function obtained by repeatedly composing $f(z) = \frac{1}{2}(z + z^{-1})$ with itself.

Definition 3.1. The *Newton iteration* for computing $\text{sign}(A)$ is given by

$$A_{j+1} = \frac{1}{2}(A_j + A_j^{-1}); \quad A_0 = A.$$

Recalling that the multiplicative “inverse” of $(B \setminus A)$ is $(A \setminus B)$, the standard Newton iteration can be applied to matrix relations as follows:

$$(B_{j+1} \setminus A_{j+1}) = \frac{1}{2}[(B_j \setminus A_j) + (A_j \setminus B_j)]; \quad (B_0 \setminus A_0) = (B \setminus A). \quad (3.3)$$

Algorithm 2 executes¹⁴ p steps of this iteration according to Theorem 1.3. Here, the factor of $\frac{1}{2}$ is applied by scaling A_{j+1} by $\frac{1}{\sqrt{2}}$ and B_{j+1} by $\sqrt{2}$, which is necessary to guarantee convergence of the individual matrices as $j \rightarrow \infty$ in exact arithmetic (see [9, Theorem 3.6]). As in the approach based on **IRS**, some post-processing is necessary to obtain $P_{R, \text{Re}(z) > 0}$, where again the subscript clarifies the corresponding subset of the spectrum of (A, B) . In this case, $B_j^{-1}A_j$ approximates $\text{sign}(B^{-1}A)$ and therefore

$$P_{R, \text{Re}(z) > 0} \approx \frac{1}{2}(B_j^{-1}A_j + I) = \frac{1}{2}B_j^{-1}(A_j + B_j). \quad (3.4)$$

Equivalently, $P_{R, \text{Re}(z) > 0}$ corresponds to the matrix relation $(2B_j \setminus (A_j + B_j))$.

As its name suggests, the Newton iteration can be viewed as an extension of classical Newton’s method, which finds roots of $z^2 - 1$ according to $z_{j+1} = \frac{1}{2}(z_j + z_j^{-1})$. Indeed, the Newton iteration for $\text{sign}(A)$ applies this version of Newton’s method to the eigenvalues of A , and quadratic convergence of classical Newton’s method implies quadratic convergence for (3.3).

3.2 (Weighted) Halley Iteration

The connection between **IF-Newton** and classical Newton’s method suggests that other approaches for computing $\text{sign}(A)$ can be obtained from alternative root finding iterations. Halley’s method, for example,

¹⁴This is not the first inverse-free implementation of the Newton iteration. In fact, Benner and Byers present their own version of **IF-Newton** [9, Algorithm 1], which incorporates scaling to promote faster convergence.

approximates roots of $z^2 - 1$ according to the third-order iteration

$$z_{j+1} = z_j \frac{z_j^2 + 3}{3z_j^2 + 1}. \quad (3.5)$$

Consequently, it implies the following iteration for $\text{sign}(A)$.

Definition 3.2. The *Halley iteration* for computing $\text{sign}(A)$ is given by

$$A_{j+1} = A_j(3A_j^2 + 1)^{-1}(A_j^2 + 3); \quad A_0 = A.$$

Recalling that any Möbius transformation can be applied to $(B \setminus A)$ for free, only two QR factorizations are required to run the Halley iteration on matrix relations if evaluated as

$$(B_{j+1} \setminus A_{j+1}) = (B_j \setminus A_j)h((B_j \setminus A_j)^2); \quad (B_0 \setminus A_0) = (B \setminus A) \quad (3.6)$$

for $h(z) = \frac{3z+1}{z+3}$. As in the Newton iteration, the approximation of $\text{sign}(z)$ corresponding to (3.6) can be obtained by repeated composition, this time with $f(z) = zh(z^2)$. Applying [Theorem 1.3](#) yields [Algorithm 3](#), which executes p steps of this Halley iteration on an arbitrary pencil (A, B) . As in **IF-Newton**, the outputs of this routine yield the projector $P_{R, \text{Re}(z) > 0}$ according to (3.4).

Algorithm 3 Inverse-Free Halley Iteration (**IF-Halley**)

Input: $A, B \in \mathbb{C}^{n \times n}$, p a number of iterations.

Requires: (A, B) has no eigenvalues on $\text{Re}(z) = 0$.

```

1:  $A_0 = A$ 
2:  $B_0 = B$ 
3: for  $i = 0 : p - 1$  do
4:    $\begin{pmatrix} -B_i \\ A_i \end{pmatrix} = \begin{pmatrix} Q_{11} & Q_{12} \\ Q_{21} & Q_{22} \end{pmatrix} \begin{pmatrix} R_i \\ 0 \end{pmatrix}$ 
5:    $C_i = Q_{12}^H A_i + 3Q_{22}^H B_i$ 
6:    $D_i = 3Q_{12}^H A_i + Q_{22}^H B_i$ 
7:    $\begin{pmatrix} -D_i \\ A_i \end{pmatrix} = \begin{pmatrix} U_{11} & U_{12} \\ U_{21} & U_{22} \end{pmatrix} \begin{pmatrix} \hat{R}_i \\ 0 \end{pmatrix}$ 
8:    $A_{i+1} = U_{12}^H C_i$ 
9:    $B_{i+1} = U_{22}^H B_i$ 
10: end for
11: return  $(A_p, B_p)$ 

```

If **IF-Halley** can exhibit third-order convergence, as we demonstrate more rigorously in the next section, is it necessarily a better choice than **IF-Newton**? In practice, the answer is no; in fact, it is likely to be less efficient in general. As a third-order method, we can expect **IF-Halley** to cut the number of iterations required by **IF-Newton** by roughly a factor of $\log_2(3)$ (in general $\log_2(m)$ for an order m iteration). Since each iteration of **IF-Halley** is twice as expensive as one of **IF-Newton**, the latter is likely to be less costly overall, despite converging more slowly.

We might hope that by modifying the Halley iteration we can overcome this drawback, guaranteeing faster convergence on at least some problems. To do this, we consider varying the Möbius transformation h , replacing (3.5) with

$$z_{j+1} = z_j \frac{a_j z_j^2 + b_j}{c_j z_j^2 + d_j} \quad (3.7)$$

for some $a_j, b_j, c_j, d_j \in \mathbb{C}$ satisfying $a_j d_j - b_j c_j \neq 0$, which are allowed to evolve with each iteration. Note that doing so will not change the complexity of the method. To streamline the choice of these coefficients, we make the following simplifications:

1. Without loss of generality, we can set $d_j = 1$ for all j .

2. Since $\text{sign}(z)$ fixes ± 1 , we enforce that the iteration does as well. This will be guaranteed as long as $c_j = a_j + b_j - 1$.

From here we obtain a specialized Indicator Approximation Problem: if we know that the spectrum of (A, B) is contained in particular subsets of S and $\mathbb{C} \setminus S$, can we choose a_j and b_j to optimally approximate $\text{sign}(z)$ on them?

A solution to this problem is already known when the spectrum of (A, B) is real and in particular lies in a union of intervals $[-1, -l_0] \cup [l_0, 1]$ for some $l_0 > 0$.¹⁵ By considering only real a_j, b_j in this case, we guarantee that eigenvalues lie in a similar union $[-1, -l_j] \cup [l_j, 1]$ at each step, where

$$l_{j+1} = \min_{l_j \leq x \leq 1} x \frac{a_j x^2 + b_j}{(a_j + b_j - 1)x^2 + 1}. \quad (3.8)$$

To promote fast convergence, we want l_j to be as close to one as possible at each iteration (see [Lemma 3.13](#)). We therefore obtain the following optimization problem.

$$\underset{a_j, b_j}{\text{maximize}} \quad l_{j+1} \quad \text{subject to} \quad a_j, b_j > 0 \quad \text{and} \quad a_j + b_j > 1. \quad (3.9)$$

Here, we require that $a_j, b_j, c_j > 0$ to ensure that $[l_j, 1] \mapsto [l_{j+1}, 1]$ guarantees also $[-1, -l_j] \mapsto [-1, -l_{j+1}]$.

Given a starting value l_0 , the solution to this optimization problem consists of the following:

$$\begin{cases} \gamma_j = \sqrt[3]{\frac{4(1-l_j^2)}{l_j^4}}; & b_j = \sqrt{1 + \gamma_j} + \frac{1}{2} \sqrt{8 - 4\gamma_j + \frac{8(2-l_j^2)}{l_j^2 \sqrt{1+\gamma_j}}}; \\ a_j = \frac{1}{4}(b_j - 1)^2; & l_{j+1} = l_j \frac{a_j l_j^2 + b_j}{(a_j + b_j - 1)l_j^2 + 1} \end{cases} \quad (3.10)$$

For this choice of a_j and b_j we note that $(a_j, b_j) \rightarrow (1, 3)$ as $l_j \rightarrow 1$, meaning the corresponding modified Halley iteration gradually approaches the standard version as it converges.

The solution (3.10) is due to Nakatsukasa, Bai, and Gygi [32], who introduced a *dynamically weighted* Halley iteration to compute the polar decomposition of a matrix. In their case, a variation of [Definition 3.2](#) converges to the (unitary) polar factor of A by driving its singular values to one. As a result, they arrive at the same optimization problem, seeking a Möbius transformation that yields a particularly accurate approximation of $\text{sign}(z)$ on a portion of the real axis (in their case just $[l_j, 1]$). While the optimized coefficients are eventually obtained via a direct and exhaustive search, a connection to the work of Zolotarev [46] was later made by Nakatsukasa and Freund [33], who demonstrated that the rational function corresponding to (3.10) can be interpreted as an optimal approximation¹⁶ to the sign function on $[-1, -l_j] \cup [l_j, 1]$ – i.e., it solves exactly our specialized Indicator Approximation Problem.

Applying (3.10) to [Algorithm 3](#) produces [Algorithm 4](#), which – borrowing terminology from Nakatsukasa, Bai, and Gygi – we call an inverse-free dynamically weighted Halley iteration (**IF-DWH**). Note that this routine requires not only that the spectrum of (A, B) is contained in a symmetric union of intervals in $[-1, 1]$ but that a lower bound l_0 on the minimum eigenvalue (in magnitude) is known.

IF-DWH is relevant for any regular matrix pencil that has (nonzero) real eigenvalues. This includes the important definite generalized eigenvalue problem, where A and B are Hermitian and the *Crawford number*

$$\gamma(A, B) = \min_{\|x\|_2=1} |x^H(A + iB)x| = \min_{\|x\|_2=1} \sqrt{(x^H A x)^2 + (x^H B x)^2} \quad (3.11)$$

is strictly positive. As a generalization of the Hermitian eigenvalue problem, definite pencils appear frequently in applications – see e.g., [19, 30].

3.3 Convergence Bounds

We close this section with a handful of convergence results. As in much of the literature for sign-function-based methods, the circles of Apollonius are the key theoretical tool.

¹⁵We assume here that zero is not an eigenvalue of (A, B) , as in that case the sign function is not defined.

¹⁶Optimal meaning the best (in the infinity norm) rational function approximation $p(x)/q(x)$ for $p(x)$ and $q(x)$ real polynomials of degree three and two, respectively.

Algorithm 4 Inverse-Free Dynamically Weighted Halley Iteration (**IF-DWH**)**Input:** $A, B \in \mathbb{C}^{n \times n}$, p a number of iterations, $l_0 > 0$.**Requires:** Eigenvalues λ of (A, B) are real with $l_0 < |\lambda| \leq 1$.

```
1:  $A_0 = A$ 
2:  $B_0 = B$ 
3: for  $j = 0 : p - 1$  do
4:    $\gamma_j = (4(1 - l_j^2)/l_j^4)^{1/3}$ 
5:    $b_j = \sqrt{1 + \gamma_j} + \frac{1}{2}\sqrt{8 - 4\gamma_j + 8(2 - l_j^2)/(l_j^2\sqrt{1 + \gamma_j})}$ 
6:    $a_j = \frac{1}{4}(b_j - 1)^2$ 
7:    $c_j = a_j + b_j - 1$ 
8:    $\begin{pmatrix} -B_j \\ A_j \end{pmatrix} = \begin{pmatrix} Q_{11} & Q_{12} \\ Q_{21} & Q_{22} \end{pmatrix} \begin{pmatrix} R_j \\ 0 \end{pmatrix}$  ▷ Apply Halley iteration
9:    $C_j = a_j Q_{12}^H A_j + b_j Q_{22}^H B_j$ 
10:   $D_j = c_j Q_{12}^H A_j + Q_{22}^H B_j$ 
11:   $\begin{pmatrix} -D_j \\ A_j \end{pmatrix} = \begin{pmatrix} U_{11} & U_{12} \\ U_{21} & U_{22} \end{pmatrix} \begin{pmatrix} \hat{R}_j \\ 0 \end{pmatrix}$ 
12:   $A_{j+1} = U_{12}^H C_j$ 
13:   $B_{j+1} = U_{22}^H B_j$ 
14:   $l_{j+1} = l_j(a_j l_j^2 + b_j)/(c_j l_j^2 + 1)$  ▷ Compute next value of  $l$ 
15: end for
16: return  $(A_p, B_p)$ , optionally  $l_p$ 
```

Definition 3.3. For $\alpha \in (0, 1)$ let

$$C_\alpha^+ = \left\{ z : \left| \frac{1-z}{1+z} \right| \leq \alpha \right\}, \quad C_\alpha^- = \left\{ z : \left| \frac{1+z}{1-z} \right| \leq \alpha \right\}$$

be sets in the right and left half planes, respectively. The boundaries ∂C_α^+ and ∂C_α^- of these sets are the *circles of Apollonius* corresponding to α .

C_α^+ can be equivalently characterized as the disk with center $\frac{1+\alpha^2}{1-\alpha^2}$ and radius $\frac{2\alpha}{1-\alpha^2}$, with C_α^- its image under a reflection across the imaginary axis. For varying α , ∂C_α^+ and ∂C_α^- define families of non-concentric circles, which collapse to the points ± 1 as $\alpha \rightarrow 0$. Since this geometric picture will be important to have in mind, [Figure 2](#) plots a handful of Apollonian circles. Throughout, we use C_α to denote the region $C_\alpha^+ \cup C_\alpha^-$.

Given their relationship to the points ± 1 , the circles of Apollonius are naturally equipped to describe convergence to the sign function. Indeed, the Newton iteration can be characterized by the following observation of Roberts [\[35\]](#).

Proposition 3.4. *The function $f(z) = \frac{1}{2}(z + z^{-1})$ defining the Newton iteration maps C_α^+ to $C_{\alpha^2}^+$ and C_α^- to $C_{\alpha^2}^-$.*

Extending this to the Halley iteration is straightforward. [Lemma 3.5](#) captures the third-order convergence of Halley's method for finding the roots of $z^2 - 1$.

Lemma 3.5. *The function $f(z) = zh(z^2) = z\frac{z^2+3}{3z^2+1}$ defining the Halley iteration maps C_α^+ to $C_{\alpha^3}^+$ and C_α^- to $C_{\alpha^3}^-$.*

Proof. Applying the definition of C_α^\pm , we have

$$\frac{1-f(z)}{1+f(z)} = \frac{1 - \frac{z^3+3z}{3z^2+1}}{1 + \frac{z^3+3z}{3z^2+1}} = \frac{3z^2 + 1 - z^3 - 3z}{3z^2 + 1 + z^3 + 3z} = \frac{(1-z)^3}{(1+z)^3}. \quad (3.12)$$

The result follows immediately. □

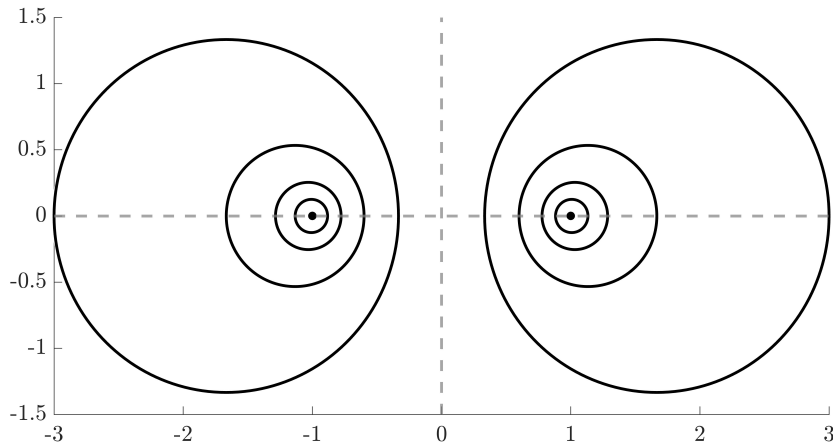


Figure 2: The circles of Apollonius corresponding to $\alpha = \frac{1}{2}, \frac{1}{4}, \frac{1}{8},$ and $\frac{1}{16}$.

Remark 3.6. The proof of [Lemma 3.5](#) implies yet another strategy for deriving iterative methods for the sign function: work backwards from $\pm \frac{(1-z)^m}{(1+z)^m}$ given a desired order of convergence m . As an example, $-\frac{(1-z)^4}{(1+z)^4}$ can be written as

$$-\frac{(1-z)^4}{(1+z)^4} = \frac{1 - \frac{1+6z^2+z^4}{4z+4z^3}}{1 + \frac{1+6z^2+z^4}{4z+4z^3}}, \quad (3.13)$$

which implies an iterative rational function

$$f(z) = \frac{1 + 6z^2 + z^4}{4z + 4z^3} = \frac{z}{4} \left(\frac{1}{z^2} + \frac{z^2 + 5}{1 + z^2} \right), \quad (3.14)$$

where the latter expression indicates that this iteration can be implemented according to [Theorem 1.3](#) with only three QR factorizations.

Remark 3.7. An alternative approach – not built on root finding – is the AAA algorithm of Nakatsukasa, Sète, and Trefethen [\[34\]](#), which has shown promise at approximating the sign function (in addition to being well-suited to the general $\mathbb{1}_S(z)$ case). A potential challenge of using the AAA algorithm is the barycentric form of the resulting rational function, which is not obviously compatible with the inverse-free arithmetic of Benner and Byers.

We can translate results like [Lemma 3.5](#) into bounds for corresponding iterative methods with one more tool: the ϵ -pseudospectrum.

Definition 3.8. For any $\epsilon > 0$, the ϵ -pseudospectrum of A is

$$\Lambda_\epsilon(A) = \{z : \text{there exists a vector } u \neq 0 \text{ with } (A + E)u = zu \text{ for some } \|E\|_2 \leq \epsilon\}.$$

The following lemma of Banks et al. [\[6, Lemma 4.3\]](#) implies that a bound on the pseudospectrum of a matrix, in terms of the circles of Apollonius, can be bootstrapped into a bound on the sign function.

Lemma 3.9 (Banks et al. 2022). *Suppose $\Lambda_\epsilon(A) \subset C_\alpha$ for some $\epsilon > 0$. Then,*

$$\|A - \text{sign}(A)\|_2 \leq \frac{8\alpha^2}{\epsilon(1+\alpha)(1-\alpha)^2}.$$

To make use of this result, we need only characterize the way our iterations transform pseudospectral bounds. The following lemma provides a general picture (and in fact specifically generalizes another result of Banks et al. [\[6, Lemma 4.4\]](#)).

Lemma 3.10. *Suppose the rational function f has all of its poles on the imaginary axis and maps $C_\alpha^\pm \rightarrow C_{\alpha^m}^\pm$ with $\partial C_\alpha^\pm \rightarrow \partial C_{\alpha^m}^\pm$ for any $\alpha \in (0, 1)$. Let f define an iteration for $\text{sign}(X)$ according to*

$$X_{k+1} = f(X_k); \quad X_0 = X.$$

If $\Lambda_\epsilon(X_k) \subset C_\alpha$, then for any $\alpha' \in (\alpha^m, \alpha)$ we have $\Lambda_{\epsilon'}(X_{k+1}) \subset C_{\alpha'}$ with

$$\epsilon' = \frac{\epsilon(1 - \alpha^2)(\alpha' - \alpha^m)}{8\alpha}.$$

Proof. Let w be any point in the “annulus” between C_α and $C_{\alpha'}$. Since f maps C_α to $C_{\alpha'}$ and $w \notin C_{\alpha'}$, the rational function $\frac{1}{w-f(z)}$ is holomorphic on C_α . Moreover, C_α contains $\Lambda(X_k)$, meaning we can bound $\|(wI - X_{k+1})^{-1}\|_2$ as

$$\begin{aligned} \|(wI - X_{k+1})^{-1}\|_2 &= \left\| \frac{1}{2\pi i} \int_{\partial C_\alpha} \frac{(w - f(z))^{-1}}{zI - X_k} dz \right\|_2 \\ &\leq \frac{1}{2\pi} \int_{\partial C_\alpha^+} \frac{\|(zI - X_k)^{-1}\|_2}{|w - f(z)|} dz + \frac{1}{2\pi} \int_{\partial C_\alpha^-} \frac{\|(zI - X_k)^{-1}\|_2}{|w - f(z)|} dz. \end{aligned} \quad (3.15)$$

Appealing to the ML-inequality, the first integral in this expression becomes

$$\begin{aligned} \int_{\partial C_\alpha^+} \frac{\|(zI - X_k)^{-1}\|_2}{|w - f(z)|} dz &\leq l(\partial C_\alpha^+) \sup_{z \in \partial C_\alpha^+} \frac{\|(zI - X_k)^{-1}\|_2}{|w - f(z)|} \\ &= \frac{4\pi\alpha}{1 - \alpha^2} \sup_{z \in \partial C_\alpha^+} \frac{\|(zI - X_k)^{-1}\|_2}{|w - f(z)|}. \end{aligned} \quad (3.16)$$

Now $\Lambda_\epsilon(X_k) \cap \partial C_\alpha^+ = \emptyset$, so $\|(zI - X_k)^{-1}\|_2 \leq \epsilon^{-1}$ for all $z \in \partial C_\alpha^+$. Using the fact that $f(z) \in C_{\alpha^m}^+$ if $z \in C_\alpha^+$, we therefore have

$$\int_{\partial C_\alpha^+} \frac{\|(zI - X_k)^{-1}\|_2}{|w - f(z)|} dz \leq \frac{4\pi\alpha}{\epsilon(1 - \alpha^2)} \sup_{y \in \partial C_{\alpha^m}^+} \frac{1}{|w - y|} \leq \frac{8\pi\alpha}{\epsilon(1 - \alpha^2)(\alpha' - \alpha^m)}, \quad (3.17)$$

where the last inequality follows from [6, Lemma 4.5]. Since we obtain the same bound on the remaining term of (3.15), we conclude

$$\|(wI - X_{k+1})^{-1}\|_2 \leq \frac{8\alpha}{\epsilon(1 - \alpha^2)(\alpha' - \alpha^m)}, \quad (3.18)$$

and therefore $w \notin \Lambda_{\epsilon'}(X_{k+1})$ for $\epsilon' = \frac{\epsilon(1 - \alpha^2)(\alpha' - \alpha^m)}{8\alpha}$. Since (3.18) applies to any point w between C_α and $C_{\alpha'}$ and $\Lambda(X_{k+1}) \subset C_{\alpha'}$, this suffices to show $\Lambda_{\epsilon'}(X_{k+1}) \subset C_{\alpha'}$. \square

In exact arithmetic, the preceding lemmas immediately extend to the case where $\text{sign}(B^{-1}A)$ is computed implicitly. Taking the place of $\Lambda_\epsilon(A)$ in the resulting error bound is the ϵ -pseudospectrum of the pencil (A, B) , defined as follows.¹⁷

Definition 3.11. For any $\epsilon > 0$, the ϵ -pseudospectrum of (A, B) is

$$\Lambda_\epsilon(A, B) = \{z : \text{there exists } u \neq 0 \text{ with } (A + E)u = z(B + F)u \text{ for some } \|E\|_2, \|F\|_2 \leq \epsilon\}.$$

Proposition 3.12 presents our main convergence result, which applies to both **IF-Newton** and **IF-Halley** (with $m = 2$ and $m = 3$, respectively) but is not specific to either. We draw a connection here to analogous results for **IRS** – i.e., [2, Theorem 1] – noting that a bound on $\|B_j^{-1}A_j - \text{sign}(B^{-1}A)\|_2$ can be bootstrapped into one for the projector $P_{R, \text{Re}(z) > 0}$ as follows:

$$\left\| \frac{1}{2}B_j^{-1}(A_j + B_j) - P_{R, \text{Re}(z) > 0} \right\|_2 = \frac{1}{2}\|B_j^{-1}A_j - \text{sign}(B^{-1}A)\|_2. \quad (3.19)$$

¹⁷There are actually many ways to define the pseudospectra of (A, B) . **Definition 3.11** is originally due to Frayssé et al. [20].

Proposition 3.12. *Let $A, B \in \mathbb{C}^{n \times n}$ and let f be a rational function satisfying the assumptions of [Lemma 3.10](#) for a corresponding value $m > 1$. Define the following inverse-free iteration for approximating $\text{sign}(B^{-1}A)$:*

$$(B_{j+1} \setminus A_{j+1}) = f(B_j \setminus A_j); \quad (B_0 \setminus A_0) = (B \setminus A).$$

If $\Lambda_\epsilon(A, B) \subset C_\alpha$ for some $\epsilon > 0$ and $\alpha \in (0, 1)$, then for any $1 < c < \alpha^{-(m-1)}$ we have

$$\|B_j^{-1}A_j - \text{sign}(B^{-1}A)\|_2 \leq \left(c^{\frac{1}{m-1}}\alpha\right)^{m^j} \cdot \frac{8\alpha\|B\|_2}{\epsilon(c-1)^2} \cdot \left[\frac{8c}{(1-\alpha^2)(c-1)}\right]^j.$$

Proof. Since $\Lambda_\epsilon(A, B)$ is bounded B is invertible.¹⁸ Consider then the explicit iteration $X_{j+1} = f(X_j)$ for $X_0 = B^{-1}A$, which in exact arithmetic is equivalent to its inverse-free counterpart. Let α_j and ϵ_j be (decreasing) sequences of parameters defined recursively as follows:

$$\begin{cases} \alpha_j = c\alpha_{j-1}^m, & \alpha_0 = \alpha \\ \epsilon_j = \frac{1}{8}\epsilon_{j-1}(1-\alpha^2)(c-1)\alpha_{j-1}^{m-1}, & \epsilon_0 = \frac{\epsilon}{\|B\|_2}. \end{cases} \quad (3.20)$$

We show inductively that $\Lambda_{\epsilon_j}(X_j) \subset C_{\alpha_j}$. The base case ($j = 0$) is trivial and follows from the observation $\Lambda_{\epsilon/\|B\|_2}(B^{-1}A) \subseteq \Lambda_\epsilon(A, B)$. Consider now arbitrary j . Plugging our induction hypothesis into [Lemma 3.10](#), and taking¹⁹ $\alpha' = \alpha_j$, we conclude that $\Lambda_{\epsilon_{j-1}}(X_{j-1}) \subset C_{\alpha_{j-1}}$ implies $\Lambda_{\epsilon'}(X_j) \subset C_{\alpha_j}$ for

$$\epsilon' = \frac{\epsilon_{j-1}(1-\alpha_{j-1}^2)(\alpha_j - \alpha_{j-1}^m)}{8\alpha_{j-1}} = \frac{\epsilon_{j-1}(1-\alpha_{j-1}^2)(c-1)\alpha_{j-1}^m}{8\alpha_{j-1}} > \frac{\epsilon_{j-1}(1-\alpha^2)(c-1)\alpha_{j-1}^m}{8} = \epsilon_j. \quad (3.21)$$

Hence, $\Lambda_{\epsilon_j}(X_j) \subset C_{\alpha_j}$. We can now bound error in the approximation via [Lemma 3.9](#). Noting that $\text{sign}(B^{-1}A) = \text{sign}(X_j)$ since X_j and $B^{-1}A$ have the same (right) eigenvectors, we have

$$\|B_j^{-1}A_j - \text{sign}(B^{-1}A)\|_2 = \|X_j - \text{sign}(X_j)\|_2 \leq \frac{8\alpha_j^2}{\epsilon_j(1+\alpha_j)(1-\alpha_j)^2} \leq \frac{8\alpha_j^2}{\epsilon_j(c-1)^2}, \quad (3.22)$$

where the last inequality follows from the bounds $1 + \alpha_j > 1$ and $|1 - \alpha_j| > c - 1$. We complete the proof by converting (3.20) into the non-recursive expressions $\alpha_j = c^{\frac{m^j-1}{m-1}}\alpha^{m^j}$ and $\epsilon_j = \frac{\epsilon\alpha_j}{\|B\|_2\alpha} \left[\frac{(1-\alpha^2)(c-1)}{8c}\right]^j$ and applying them to (3.22). To simplify, note that

$$c^{\frac{m^j-1}{m-1}}\alpha^{m^j} = \left[c^{\frac{m^j-1}{m-1}}\alpha\right]^{m^j} \leq \left[c^{\frac{1}{m-1}}\alpha\right]^{m^j} \quad (3.23)$$

for any j . □

In the setting where $B = I$ and f is the rational function defining the standard Newton iteration, so that $m = 2$, [Proposition 3.12](#) reduces to [[6](#), Proposition 4.8]. As mentioned in its proof, our result implicitly assumes that B is invertible via the pseudospectral bound $\Lambda_\epsilon(A, B) \subset C_\alpha$, though this is of course necessary for $\text{sign}(B^{-1}A)$ to be defined.

For **IF-DWH**, we can state an alternative and somewhat simpler result for definite pencils, which does not involve the pseudospectrum. Nevertheless, assuming that $\Lambda(A, B)$ is bounded again implies that B must be invertible.

Lemma 3.13. *Suppose (A, B) is a definite pencil with eigenvalues in $(-1, -l_0) \cup (l_0, 1)$ and let $[A_j, B_j, l_j] = \text{IF-DWH}(A, B, j, l_0)$. Then*

$$\|B_j^{-1}A_j - \text{sign}(B^{-1}A)\|_2 \leq \frac{\|(A, B)\|_2}{\gamma(A, B)}(1 - l_j).$$

¹⁸In fact, $\Lambda_\epsilon(A, B)$ is bounded if and only if $\sigma_n(B) > \epsilon$.

¹⁹Note that the restriction $c < \alpha^{-(m-1)}$ guarantees $\alpha_j \in (\alpha_{j-1}^m, \alpha_{j-1})$ for any j .

Proof. Let X be the invertible eigenvector matrix of (A, B) satisfying

$$(X^H A X, X^H B X) = (\Lambda_A, \Lambda_B) = (\text{diag}(\alpha_1, \dots, \alpha_n), \text{diag}(\beta_1, \dots, \beta_n)) \quad (3.24)$$

for $\alpha_i, \beta_i \in \mathbb{R}$ with $\alpha_i^2 + \beta_i^2 = 1$, which exists since (A, B) is definite (see [41, Chapter VI]). Since (A_j, B_j) has the same right eigenvectors as (A, B) , X diagonalizes $B_j^{-1} A_j$. Writing $B_j^{-1} A_j = X \Lambda_j X^{-1}$ for Λ_j diagonal and noting $B^{-1} A = X \Lambda_B^{-1} X^H X^{-H} \Lambda_A X^{-1} = X \Lambda_B^{-1} \Lambda_A X^{-1}$, we have

$$\begin{aligned} \|B_j^{-1} A_j - \text{sign}(B^{-1} A)\|_2 &= \|X \Lambda_j X^{-1} - X \text{sign}(\Lambda_B^{-1} \Lambda_A) X^{-1}\|_2 \\ &\leq \kappa_2(X) \|\Lambda_j - \text{sign}(\Lambda_B^{-1} \Lambda_A)\|_2 \\ &\leq \kappa_2(X) (1 - l_j), \end{aligned} \quad (3.25)$$

where the last inequality follows from $\Lambda(A_p, B_p) \subseteq (-1, -l_j) \cup (l_j, 1)$. We complete the proof by noting that the specific eigenvector matrix X satisfies $\kappa_2(X) \leq \frac{\|(A, B)\|_2}{\gamma(A, B)}$ [17, Proof of Theorem 2.3]. \square

The theoretical bounds derived above imply, as we should expect, that convergence of sign-function-based methods is dependent on both the locations of the eigenvalues of (A, B) – relative to ± 1 – and the conditioning of its eigenvectors. The latter is present implicitly in Proposition 3.12 and Lemma 3.13 via the pseudospectrum and the Crawford number, respectively.

Moreover, we can now describe the set of problems for which the methods considered in this section are fast, which – as mentioned in Section 1 – means they require at most $O(\log(\frac{n}{\delta}) T_{\text{MM}}(n))$ operations to compute a projector to forward error δ in the spectral norm. As each of our algorithms is iterative, with one iteration requiring $O(T_{\text{MM}}(n))$ operations, they are fast as long as forward error falls below δ after $O(\log(\frac{n}{\delta}))$ steps. Proposition 3.12 implies that this is the case for sign-function-based methods (in exact arithmetic) when $1 - \alpha$ and ϵ are at least polynomial in δ and n^{-1} .

Since $\Lambda_\epsilon(A, B) \cap \{z : |z| = 1\} = \emptyset$ implies $d_{(A, B)} \geq 2\epsilon$, [2, Theorem 1] tells a similar story for **IRS**. Together, these results suggest a general guideline: recalling our main problem statement from Section 1, fast approximations to P_R and P_L are accessible via our computational framework provided $\Lambda_\epsilon(A, B)$ is well-separated from the boundary of S for ϵ not too small (at least polynomial in n^{-1} and the desired accuracy).

4 Numerical Examples

In this section, we present a handful of numerical examples to explore the empirical performance of **IRS**, **IF-Newton**, **IF-Halley**, and **IF-DWH**. All results were obtained in Matlab R2024a. Further examples are given in Appendix C.

Our first test is a 500×500 pencil

$$(A, B) = (X^H \Lambda X, X^H X), \quad (4.1)$$

where X is invertible and Λ is diagonal. We set

$$\Lambda = \begin{pmatrix} \Lambda_+ & 0 \\ 0 & \Lambda_- \end{pmatrix} \quad (4.2)$$

for $\Lambda_+, \Lambda_- \in \mathbb{R}^{250 \times 250}$ with diagonal entries sampled from $\mathbb{R}_{>0}$ and $\mathbb{R}_{<0}$, respectively. By construction, the eigenvalues of (A, B) belong to the diagonal of Λ , and the columns of X^{-1} are right eigenvectors. We choose real eigenvalues here to test the potential improved convergence of **IF-DWH**; in this case, the pencil (A, B) is definite.

The benefit of this construction is that it allows us to vary both the locations of the eigenvalues of (A, B) as well as the conditioning of its eigenvectors. We consider in particular the following:

- Well-separated eigenvalues: diagonal entries of Λ are sampled uniformly from $(-4, -1) \cup (1, 4)$. Well-separated here refers to distance from the imaginary axis *not* spacing between individual eigenvalues.

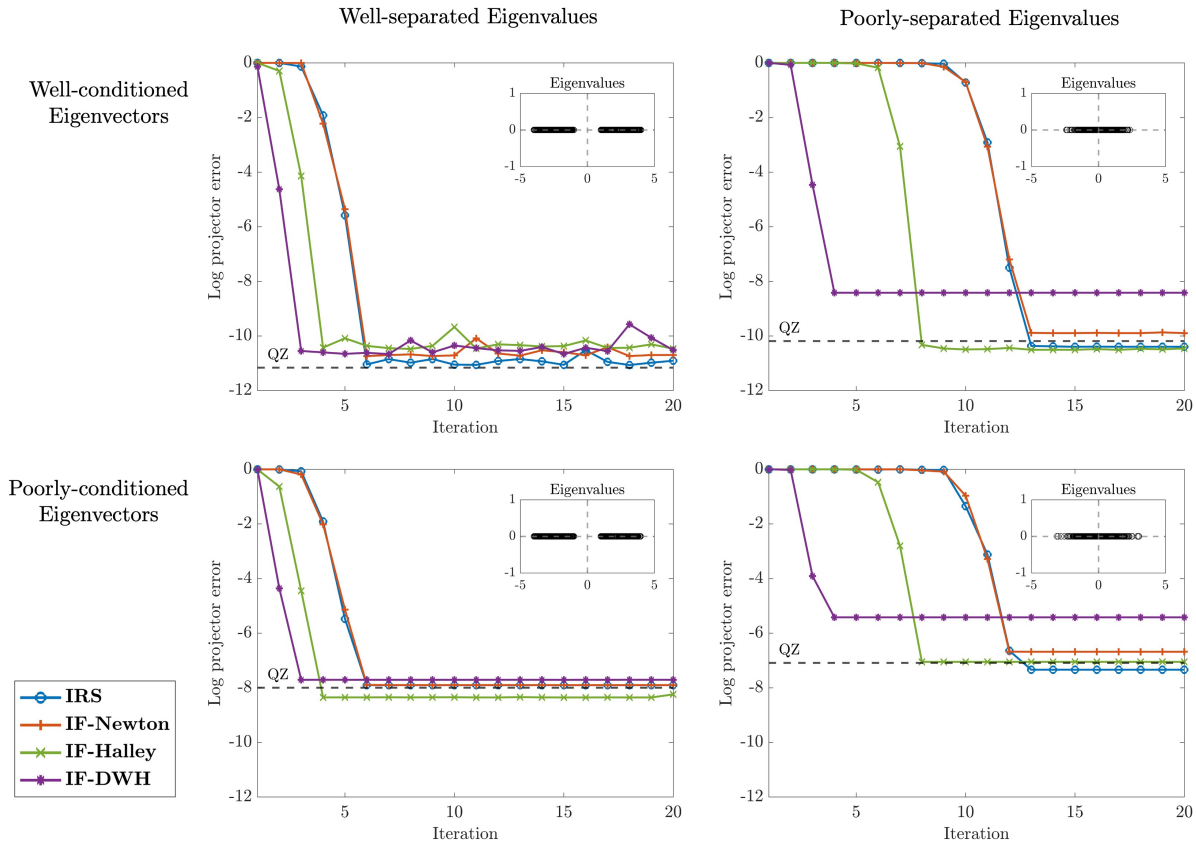


Figure 3: Forward error for **IRS**, **IF-Newton**, **IF-Halley**, and **IF-DWH** when used to compute a projector onto a deflating subspace of a 500×500 pencil (A, B) constructed according to (4.1) and (4.2). The four plots correspond to different eigenvalue/eigenvector constructions.

- Poorly-separated eigenvalues: diagonal entries of Λ_+ and Λ_- are sampled from $|\mathcal{N}(0, 1)|$ and $-\mathcal{N}(0, 1)$, respectively.
- Well-conditioned eigenvectors: X is a standard, complex Gaussian random matrix.
- Poorly-conditioned eigenvectors: X is drawn randomly (again standard, complex Gaussian) and modified so that $\kappa_2(X) = 10^5$. This is done by computing a full SVD of X and subtracting off an appropriate rank-one matrix.

Suppose we are interested in computing a unitary projector P onto the right deflating subspace of (A, B) corresponding to the right half plane (equivalently, corresponding to the eigenvalues in Λ_+). A stand-in for this projector can be obtained (without using matrix inversion) by computing an RQ factorization $X = RQ$ and taking $P = WW^H$ for W containing the first 250 columns of Q^H . Hence, we can compute the “exact” projector P without incurring significant error for either choice of X and any set of eigenvalues.

In combination with the **GRURV** algorithm of Ballard et al. [4], each of the iterative methods considered in this paper can also produce an approximation of P . At a given iteration, each method yields a pencil (A_j, B_j) with eigenvalues close to zero or one. An approximate projector can then be obtained as $\tilde{P} = UU^H$ for U a matrix containing the first 250 columns of the U-factor produced by **GRURV** when applied to $\frac{1}{2}B_j^{-1}(A_j + B_j)$ or – in the case of **IRS** – $(A_j + B_j)^{-1}A_j$. Note that in this approach, **IRS** must apply an initial Möbius transformation mapping the imaginary axis to the unit circle.

Figure 3 presents the associated forward projector error $\log_{10}(\|P - \tilde{P}\|_2)$ for each method and all four combinations of eigenvalue placement and eigenvector conditioning. Since forward error is fairly strict, we mark on each plot the accuracy of the standard QZ algorithm [31], which can approximate P by computing

	IRS	IF-Newton	IF-Halley	IF-DWH
QR's per iteration	1	1	2	2
MM's per iteration	2	3	4	4

Table 2: Number of full $2n \times n$ QR factorizations and $n \times n$ matrix multiplications required for one iteration of each method considered in this paper.

first a full eigendecomposition (by way of Schur form) and then a QR factorization of corresponding eigenvectors. This provides a benchmark for the error produced by a backward-stable method; the gap between this error and machine precision can be explained by classical error bounds (see e.g., [24, 40]).

Two trends jump out from these plots: (1) eigenvalues near the imaginary axis drive up the number of iterations required by all of the methods to converge and (2) eigenvector conditioning impacts attainable forward error but not convergence. With the exception of **IF-DWH**, each of the iterative methods is capable of matching the error produced by QZ, which recall requires an expensive full eigendecomposition.

The backdrop for this comparison is Table 2, which records the cost of each iteration of **IRS**, **IF-Newton**, **IF-Halley**, and **IF-DWH**. We are reminded here that each iteration of the Halley-type methods is roughly twice as expensive as one of **IRS** or **IF-Newton**. Hence, to be more efficient overall **IF-Halley** and **IF-DWH** must converge in fewer than half the number of iterations. **IF-Halley** cannot reach this benchmark; instead, it cuts the number of iterations by roughly a factor of $\log_2(3)$, as expected.

IF-DWH, on the other hand, converges not only faster than **IF-Halley** but fast enough to be more efficient than **IRS** or **IF-Newton**. Despite this, it is also the least accurate by a decent margin. While all of the methods stagnate on the harder problems – a sign that the variance in iterations beyond a certain point is masked by the larger forward error – **IF-DWH** does so without reaching the QZ benchmark, particularly when eigenvalues are close to the imaginary axis.

This is likely due to inherent instability in the weighted iteration. When l_0 , or more generally l_j , is small (as is the case in the first few steps of the poorly-separated plots of Figure 3), the weights in (3.7) are unbalanced in the sense that a_j, b_j , and c_j are large while $d_j = 1$. As a result, the input to the second QR factorization computed by **IF-DWH** (line 11 in Algorithm 4) is potentially ill-conditioned, specifically if $Q_{12}^H A_j$ is itself ill-conditioned. When this occurs, significant error is incurred after only one iteration, enough to move **IF-DWH** away from the error achieved by the other methods. Interestingly, this phenomenon was not reported in the original version of the dynamically weighted Halley iteration [32] and is possibly specific to our general, inverse-free implementation.

To overcome this drawback, we suggest simply using a modified Halley iteration: if l_0 is initially small (recall that l_0 is an input for **IF-DWH**) run a few standard Halley iterations – i.e., **IF-Halley** – before switching to **IF-DWH**. The result is a method that converges somewhere in between **IF-DWH** and **IF-Halley**; when the gap between the two is significant, this modified iteration can both avoid the error stagnation of **IF-DWH** while converging fast enough to beat **IRS** and **IF-Newton**.

We verify this in Figure 4, which presents the same log projector error for this modified iteration with different numbers of initial Halley steps. Since the poor performance of **IF-DWH** appeared independent of eigenvector conditioning in Figure 3, we consider here a version of (4.1) where X is Haar unitary, in which case P can be obtained exactly from the leading columns of X . As anticipated, the modified iteration does progressively better as the number of initial Halley iterations is increased. In both plots of Figure 5 these methods also converge in fewer than half the iterations of **IRS** and **IF-Newton**, as desired.

More testing is necessary to provide rigorous guidelines for choosing the number of standard Halley iterations to run before defaulting to **IF-DWH**. It may also be worth initially running one of the second order methods instead of **IF-Halley** to further save on computational costs.

In Appendix C we present additional examples. Figure 5 verifies the improved convergence of **IF-DWH** on problems with real eigenvalues while Figure 6 demonstrates the advantages of avoiding matrix inversion.

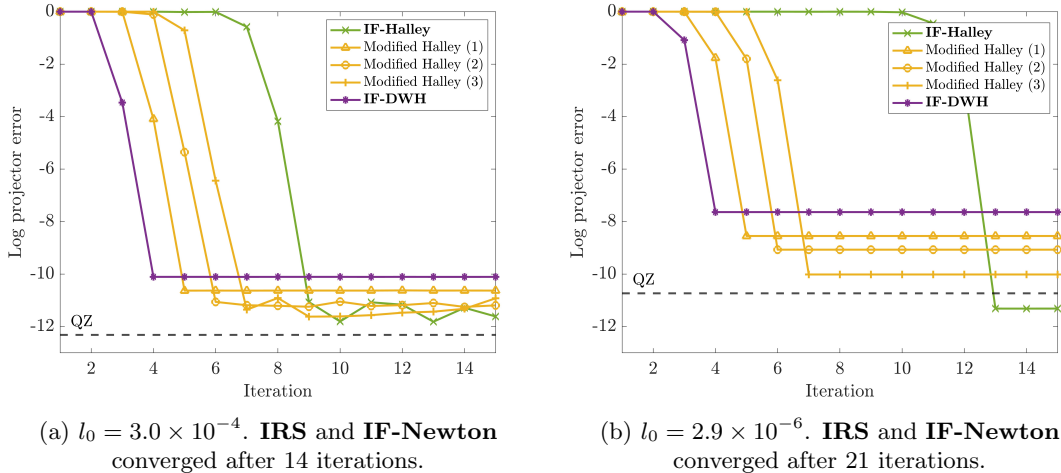


Figure 4: Forward projector error for methods based on the Halley iteration. The input pencil (A, B) is again 500×500 constructed according to (4.1), this time with a Haar unitary eigenvector matrix X . Two (real) eigenvalue placements are considered with the corresponding input value of l_0 listed. For each modified iteration, we note in parentheses the number of standard Halley steps applied before switching to the weighted version. For context, we also include the number of iterations required by **IRS** and **IF-Newton**; to be more efficient overall, a Halley-based method must converged in fewer than half as many.

5 Conclusion

This paper presented a high-level, inverse-free framework for computing the spectral projectors of any regular matrix pencil (A, B) . We used this framework to state a number of new iterative methods for the problem, providing theoretical and empirical evidence for their efficacy. In doing so, we have also reinforced the practical value of the high-level framework and its accompanying Indicator Approximation Problem. For practitioners looking to handle this fundamental problem in numerical linear algebra without relying on inversion, our work offers a wealth of new options.

6 Acknowledgements

This work was supported by Graduate Fellowships for STEM Diversity (GFSD) and the following NSF grants: DMS-2154099, FRG award DMS-1952786, and MSPRF 2402027. Special thanks to Yuji Nakatsukasa for suggesting the function approximation perspective as well as Volker Mehrmann for helpful correspondence. Note that a majority of this work was completed while the corresponding author was at UC San Diego.

References

- [1] N. Akar. A matrix analytical method for the discrete time Lindley equation using the generalized Schur decomposition. In *Proceeding from the 2006 Workshop on Tools for Solving Structured Markov Chains, SMCtools '06*, New York, NY, USA, 2006. Association for Computing Machinery.
- [2] Z. Bai, J. Demmel, and M. Gu. An inverse free parallel spectral divide and conquer algorithm for nonsymmetric eigenproblems. *Numerische Mathematik*, 76:279–308, 1997.
- [3] G. Ballard, J. Demmel, and I. Dumitriu. Minimizing Communication for Eigenproblems and the Singular Value Decomposition. Technical Report UCB/EECS-2011-14, EECS Department, University of California, Berkeley, Feb 2011.

- [4] G. Ballard, J. Demmel, I. Dumitriu, and A. Rusciano. A generalized randomized rank-revealing factorization. arXiv:1909.06524, 2019.
- [5] G. Ballard, J. Demmel, O. Holtz, and O. Schwartz. Minimizing Communication in Numerical Linear Algebra. *SIAM Journal on Matrix Analysis and Applications*, 32(3):866–901, 2011.
- [6] J. Banks, J. Garza-Vargas, A. Kulkarni, and N. Srivastava. Pseudospectral Shattering, the Sign Function, and Diagonalization in Nearly Matrix Multiplication Time. *Foundations of Computational Mathematics*, 23:1959–2047, 2023.
- [7] A. Beavers and E. Denman. A new similarity transformation method for eigenvalues and eigenvectors. *Mathematical Biosciences*, 21(1):143–169, 1974.
- [8] P. Benner and R. Byers. Evaluating products of matrix pencils and collapsing matrix products. *Numerical Linear Algebra with Applications*, 8(6-7):357–380, 2001.
- [9] P. Benner and R. Byers. An arithmetic for matrix pencils: Theory and new algorithms. *Numerische Mathematik*, 103:539–573, 2006.
- [10] A. Y. Bulgakov and S. Godunov. Circular dichotomy of the spectrum of a matrix. *Siberian Mathematical Journal*, 29:734–744, 1988.
- [11] D. Coppersmith and S. Winograd. Matrix multiplication via arithmetic progressions. *Journal of Symbolic Computation*, 9(3):251–280, 1990.
- [12] J. Demmel, I. Dumitriu, and O. Holtz. Fast linear algebra is stable. *Numerische Mathematik*, 108:59–91, 2007.
- [13] J. Demmel, I. Dumitriu, O. Holtz, and R. Kleinberg. Fast matrix multiplication is stable. *Numerische Mathematik*, 106, 2006.
- [14] J. Demmel, I. Dumitriu, and R. Schneider. Generalized Pseudospectral Shattering and Inverse-Free Matrix Pencil Diagonalization. arXiv:2306.03700, 2023.
- [15] J. Demmel and B. Kågström. The generalized Schur decomposition of an arbitrary pencil $A-\lambda B$ — robust software with error bounds and applications. Part I: theory and algorithms. *ACM Trans. Math. Softw.*, 19(2):160–174, 1993.
- [16] J. Demmel and B. Kågström. The generalized Schur decomposition of an arbitrary pencil $A-\lambda B$ — robust software with error bounds and applications. Part II: software and applications. *ACM Trans. Math. Softw.*, 19(2):175–201, 1993.
- [17] L. Elsner and J. Sun. Perturbation theorems for the generalized eigenvalue problem. *Linear Algebra and its Applications*, 48:341–357, 1982.
- [18] E. Evert, M. Vandecappelle, and L. De Lathauwer. Canonical Polyadic Decomposition via the Generalized Schur Decomposition. *IEEE Signal Processing Letters*, 29:937–941, 2022.
- [19] B. Ford and G. Hall. The generalized eigenvalue problem in quantum chemistry. *Computer Physics Communications*, 8(5):337–348, 1974.
- [20] V. Frayssé, M. Gueury, F. Nicoud, and V. Toumazou. Spectral portraits for matrix pencils. Technical Report, CERFACS, 1996.
- [21] J. D. Gardiner and A. J. Laub. A generalization of the matrix-sign-function solution for algebraic Riccati equations. *International Journal of Control*, 44(3):823–832, 1986.
- [22] N. J. Higham. *Accuracy and Stability of Numerical Algorithms*. Society for Industrial and Applied Mathematics, Second edition, 2002.

- [23] N. J. Higham. The scaling and squaring method for the matrix exponential revisited. *SIAM Review*, 51(4):747–764, 2009.
- [24] B. Kågström and P. Poromaa. Computing Eigenspaces with Specified Eigenvalues of a Regular Matrix Pair (A, B) and Condition Estimation: Theory, Algorithms and Software. *Numerical Algorithms*, 12:369–407, 1996.
- [25] A. N. Malyshev. Computing invariant subspaces of a regular linear pencil of matrices. *Siberian Mathematical Journal*, 30:559–567, 1989.
- [26] A. N. Malyshev. Guaranteed accuracy in spectral problems of linear algebra. *Trudy Instituta Matematiki Sibirskogo Otdeleniya AN SSSR*, 17:19–104, 1990.
- [27] A. N. Malyshev. Guaranteed accuracy in spectral problems of linear algebra. I. *Siberian Advances in Mathematics*, 2(1):144–197, 1992.
- [28] A. N. Malyshev. Guaranteed accuracy in spectral problems of linear algebra. II. *Siberian Advances in Mathematics*, 2(2):153–204, 1992.
- [29] A. N. Malyshev. Parallel algorithm for solving some spectral problems of linear algebra. *Linear Algebra and its Applications*, 188-189:489–520, 1993.
- [30] O. Mangasarian and E. Wild. Multisurface proximal support vector machine classification via generalized eigenvalues. *IEEE Transactions on Pattern Analysis and Machine Intelligence*, 28(1):69–74, 2006.
- [31] C. B. Moler and G. W. Stewart. An algorithm for generalized matrix eigenvalue problems. *SIAM Journal on Numerical Analysis*, 10(2):241–256, 1973.
- [32] Y. Nakatsukasa, Z. Bai, and F. Gygi. Optimizing Halley’s Iteration for Computing the Matrix Polar Decomposition. *SIAM Journal on Matrix Analysis and Applications*, 31(5):2700–2720, 2010.
- [33] Y. Nakatsukasa and R. W. Freund. Computing Fundamental Matrix Decompositions Accurately via the Matrix Sign Function in Two Iterations: The Power of Zolotarev’s Functions. *SIAM Review*, 58(3):461–493, 2016.
- [34] Y. Nakatsukasa, O. Sète, and L. N. Trefethen. The AAA Algorithm for Rational Approximation. *SIAM Journal on Scientific Computing*, 40(3):A1494–A1522, 2018.
- [35] J. D. Roberts. Linear model reduction and solution of the algebraic Riccati equation by use of the sign function. *International Journal of Control*, 32(4):677–687, 1980.
- [36] R. Schneider. Pseudospectral Divide-and-Conquer for the Generalized Eigenvalue Problem. PhD Thesis, 2024.
- [37] R. Shah. Fast Hermitian Diagonalization with Nearly Optimal Precision. arXiv:2408.09880, 2024.
- [38] A. Sobczyk, M. Mladenović, and M. Luisier. Invariant subspaces and PCA in nearly matrix multiplication time. arXiv:2311.10459, 2024.
- [39] G. W. Stewart. On the Sensitivity of the Eigenvalue Problem $Ax = \lambda Bx$. *SIAM Journal on Numerical Analysis*, 9(4):669–686, 1972.
- [40] G. W. Stewart. Error and Perturbation Bounds for Subspaces Associated with Certain Eigenvalue Problems. *SIAM Review*, 15(4):727–764, 1973.
- [41] G. W. Stewart and J. Sun. *Matrix Perturbation Theory*. Computer Science and Scientific Computing. Elsevier Science, 1990.
- [42] V. Strassen. Gaussian elimination is not optimal. *Numerische Mathematik*, 13:354–356, 1969.
- [43] J.-G. Sun. Perturbation bounds for the Cholesky and QR factorizations. *BIT Numerical Mathematics*, 31(2):341–352, 1991.

- [44] V. V. Williams. Multiplying Matrices Faster than Coppersmith-Winograd. In *Proceedings of the Forty-Fourth Annual ACM Symposium on Theory of Computing*, STOC '12, page 887–898. Association for Computing Machinery, 2012.
- [45] V. V. Williams, Y. Xu, Z. Xu, and R. Zhou. New bounds for matrix multiplication: from alpha to omega. arXiv:2307.07970, 2023.
- [46] Y. I. Zolotarev. Application of elliptic functions to questions of functions deviating least and most from zero. *Zap. Imp. Akad. Nauk.*, 30:1–59, 1877.

A Fast Generalized Schur Decomposition

In this appendix, we verify that the pseudospectral divide-and-conquer approach of [14] can be adapted to produce the generalized Schur decomposition of any pencil (A, B) . The result is an inverse-free and randomized algorithm that can produce an approximate Schur decomposition, of arbitrarily small backward error, in nearly matrix multiplication time.

We start by recalling the necessary theory from linear algebra. The generalized Schur decomposition of (A, B) , as introduced by Stewart [39], takes the form

$$(A, B) = Q_L(T_A, T_B)Q_R^H \tag{A.1}$$

for Q_L, Q_R unitary and T_A, T_B upper triangular. It is easy to see from (A.1) that any set of leading columns of Q_R span a right deflating subspace of (A, B) . Moreover, leading columns of Q_L span the corresponding left deflating subspaces. When (A, B) is regular, its eigenvalues are encoded as ratios of the diagonal entries of T_A and T_B , with zeros on the diagonal of T_B corresponding to eigenvalues at infinity. Eigenvectors, meanwhile, can be computed from (A.1) via cheap triangular solves.

To set the stage for a fast Schur decomposition, we first describe **EIG**, the main divide-and-conquer routine used in [14]. This algorithm block diagonalizes the input pencil recursively, at each step searching for a dividing line that splits the spectrum and subsequently computing bases for the corresponding pairs of deflating subspaces (the matrices $U_R^{(1)}, U_L^{(1)}, U_R^{(2)}$ and $U_L^{(2)}$ from Section 1). Efficiency is derived from the fact that a split separating at least a fifth of the eigenvalues can be found at each step, which is a consequence of assuming that the input pencil is suitably well-behaved – i.e., it satisfies a certain guarantee of *pseudospectral shattering* as originally defined by Banks et al. [6]. As we discuss in more detail below, and was proved rigorously in [14, Section 3], such a guarantee can be obtained for arbitrary (A, B) by applying small random perturbations to the matrices, allowing us to use **EIG** to approximately diagonalize any pencil (in the backward-error sense).

Intuitively, we can adapt this approach to obtain the Schur form of (A, B) by block upper triangularizing the pencil at each step. This requires only half the work of the diagonalization case, as we need only compute $U_R^{(1)}, U_L^{(1)} \in \mathbb{C}^{n \times k}$. Indeed, if $U_R, U_L \in \mathbb{C}^{n \times n}$ are unitary matrices such that

$$U_R = \begin{pmatrix} U_R^{(1)} & W_R \end{pmatrix}, \quad U_L = \begin{pmatrix} U_L^{(1)} & W_L \end{pmatrix} \tag{A.2}$$

for some $W_R, W_L \in \mathbb{C}^{(n-k) \times n}$, then

$$U_L^H A U_R = \begin{pmatrix} A_{11} & A_{12} \\ 0 & A_{22} \end{pmatrix}, \quad U_L^H B U_R = \begin{pmatrix} B_{11} & B_{12} \\ 0 & B_{22} \end{pmatrix}. \tag{A.3}$$

This follows from the observation that the lower left block of $U_L^H A U_R$ is $W_L^H A U_R^{(1)}$; since $A U_R^{(1)}$ belongs to the left deflating subspace of (A, B) spanned by the columns of $U_L^{(1)}$ – and moreover $\text{range}(W_L)$ is the orthogonal complement of this deflating subspace since U_L is unitary – we have $W_L^H A U_R^{(1)} = 0$. The same argument implies $W_L^H B U_R^{(1)} = 0$.

Before stating a divide-and-conquer Schur algorithm that leverages this observation, we pause to recap pseudospectral shattering. Let the grid $g = \text{grid}(z_0, \omega, s_1, s_2)$ be the boundary of the $s_1 \times s_2$ lattice in the complex plane consisting of $(\omega \times \omega)$ -sized squares with lower left corner $z_0 \in \mathbb{C}$ (and grid lines parallel

to the real/complex axis). Recalling [Definition 3.11](#), we say that $\Lambda_\epsilon(A, B)$ is *shattered* with respect to g if the following conditions hold: (1) each eigenvalue of (A, B) belongs to a unique grid box of g and (2) $\Lambda_\epsilon(A, B) \cap g = \emptyset$. As mentioned above, this definition is originally due to Banks et al. [\[6\]](#).

The key insight of [\[14\]](#) – which generalizes [\[6\]](#) – is that small, Gaussian perturbations to A and B guarantee shattering with high probability for any input pencil and a certain choice of ϵ and g (see [\[14, Theorem 3.12\]](#)). Shattering positions us perfectly for divide-and-conquer; the grid provides a collection of viable splitting lines, each guaranteed to be minimally well-separated (in the sense of [Section 3](#)) from a certain pseudospectrum of the perturbed problem, and we are also guaranteed that one of these lines splits off at least a fifth of the eigenvalues. Running divide-and-conquer over this shattering grid efficiently produces a diagonalization (or in our case a Schur decomposition) of the perturbed pencil, which can approximate the original problem (A, B) provided the initial perturbation is small.

Of course, establishing a shattering grid first requires localizing the eigenvalues in a certain disk around the origin. For the generalized eigenvalue problem in particular, this requires some care. While in the single-matrix case we can simply scale the input matrix appropriately, a pencil (A, B) can have arbitrarily large eigenvalues regardless of $\|A\|_2$ and $\|B\|_2$. Hence, the proof of shattering in [\[14\]](#) requires not only Gaussian perturbations to A and B but a scaling factor that is polynomial in the size of the pencil (and is applied to only one of the matrices); that is, shattering is proved for the pencil $(\tilde{A}, n^\alpha \tilde{B})$, where $\alpha > 1$ is a constant and \tilde{A} and \tilde{B} are obtained from A and B , respectively, by applying Gaussian perturbations. Accordingly, **EIG** assumes that the input matrices satisfy norm bounds in terms of n^α . As discussed in [\[14, Section 6\]](#), this scaling factor is primarily a theoretical necessity and can likely be dropped in practice.

We are now ready to present **SCHUR** ([Algorithm 5](#)), a version of **EIG** that produces a Schur decomposition instead of a full diagonalization. As in the diagonalization case, **SCHUR** assumes that the input pencil comes with a guarantee of pseudospectral shattering for a corresponding ϵ and grid g . Nevertheless, this routine is somewhat more general. In particular, we no longer build in the n^α scaling, instead taking an input $C > 0$ such that $\|A\|_2, \|B\|_2 \leq C$. While we will eventually set $C = 3n^\alpha$ to obtain a decomposition for arbitrary inputs, this allows the parameters of **SCHUR** to be relaxed if a better bound is available (e.g., for problems where shattering can be established without the polynomial scaling).

Throughout, **SCHUR** leverages the **GRURV** algorithm of Ballard et al. to (implicitly) compute rank-revealing factorizations of spectral projectors approximated by **IRS**.²⁰ A version of divide-and-conquer for Schur form built on these subroutines was originally proposed as **RGNEP** by Ballard, Demmel, and Dumitriu [\[3\]](#), though without the key step of pseudospectral shattering. Note that performance guarantees for **GRURV** can be found in [\[4\]](#).

Theorem A.1. *Let (A, B) and g be a pencil and grid satisfying the requirements of [Algorithm 5](#) for corresponding $\epsilon > 0$ and $C > 0$. For any $\theta \in (0, 1)$ and $\eta > 0$, suppose*

$$[Q_R, Q_L, T_A, T_B] = \text{SCHUR}(n, A, B, \epsilon, C, g, \eta, \theta)$$

in exact arithmetic. With probability at least $1 - \theta$ this call is successful – meaning its recursive procedure converges – and moreover the outputs satisfy

$$\|A - Q_L T_A Q_R^H\|_2 \leq \eta \quad \text{and} \quad \|B - Q_L T_B Q_R^H\|_2 \leq \eta.$$

Proof. We follow closely the proof of [\[14, Theorem 4.8\]](#), which exhibits success for **EIG**. Note that, in terms of our more general parameters, **EIG** takes $C = 3n^\alpha$ and $r = 5$, where r bounds (in magnitude) the imaginary and real parts of the grid points of g . In repeating the analysis of [\[14\]](#), we tighten a few inequalities where convenient and discard **EIG**'s second constraint on p – i.e., that $p \geq \log_2(\frac{105n^\alpha}{\epsilon} - 1)$ – as it is redundant.

The first few steps of the proof carry over directly: pseudospectral shattering guarantees that the pencil (A, B) in line 8 is minimally well-conditioned for repeated squaring and consequently that the choice of p in line 6 ensures that **IRS** approximates projectors to accuracy δ in the spectral norm. Similarly, we know that a good eigenvalue split always exists, and – by requiring that k is computed correctly for every grid line checked – **SCHUR** finds such a split with probability at least $1 - \frac{\theta}{10n^4}$, provided $\delta \leq \frac{\theta}{2(\theta + 10n^6\zeta)}$.

The first deviation from the diagonalization case occurs in lines 15-17, where **SCHUR** computes bases

²⁰Repeated squaring could of course be replaced by any other inverse-free method considered in this paper, provided line 8 of [Algorithm 5](#) is adjusted accordingly.

Algorithm 5 Divide-and-Conquer Generalized Schur Decomposition (**SCHUR**)

Input: $n \in \mathbb{N}_+$, $A, B \in \mathbb{C}^{m \times m}$, $\epsilon > 0$, $C > 0$, $g \subset \{z : |\operatorname{Re}(z)|, |\operatorname{Im}(z)| < r\}$ an $s_1 \times s_2$ grid of box size ω , $\eta > 0$ a desired accuracy, and $\theta \in (0, 1)$ a failure probability.

Requires: $m \leq n$, $\|A\|_2, \|B\|_2 \leq C$, and $\Lambda_\epsilon(A, B)$ shattered with respect to g .

Output: Unitary Q_R, Q_L and an upper triangular pencil (T_A, T_B) such that $\|A - Q_L T_A Q_R^H\|_2 \leq \eta$ and $\|B - Q_L T_B Q_R^H\|_2 \leq \eta$ with probability at least $1 - \theta$ (see [Theorem A.1](#)).

```
1: if  $m = 1$  then
2:    $Q_R = Q_L = 1$ ;  $T_A = A$ ;  $T_B = B$ 
3: else
4:    $\zeta = 2(\lceil \log_2(\max\{s_1, s_2\}) + 1 \rceil)$ 
5:    $\delta = \min \left\{ \frac{\theta}{2(\theta + 10n^6\zeta)}, \sqrt{\frac{\theta}{5}} \frac{1}{n^3 C^2} \min \left\{ \frac{\epsilon^2}{800}, \frac{\eta^2}{96} \right\} \right\}$ 
6:    $p = \left\lceil \max \left\{ 7, -2 \log_2 \left( -\frac{1}{2} \log_2 \left( 1 - \frac{\epsilon}{r(1+r)C} \right) \right), 1 + \log_2 \left[ \frac{\log_2 \left( \frac{\delta \pi \epsilon}{4m\omega C + \delta \pi \epsilon} \right)}{\log_2 \left( 1 - \frac{\epsilon}{r(1+r)C} \right)} \right] \right\} \right\rceil$ 
7:   Choose a grid line  $\operatorname{Re}(z) = h$  of  $g$ 
8:    $(\mathcal{A}, \mathcal{B}) = (A - (h-1)B, A - (h+1)B)$ 
9:    $[A_p, B_p] = \mathbf{IRS}(\mathcal{A}, \mathcal{B}, p)$ 
10:   $[U, R_1, R_2, V] = \mathbf{GRURV}(2, A_p + B_p, A_p, -1, 1)$ 
11:   $k = \# \left\{ i : \left| \frac{R_2(i, i)}{R_1(i, i)} \right| \geq \sqrt{\frac{\theta}{10\zeta}} \frac{1-\delta}{n^3} \right\}$ 
12:  if  $k < \frac{1}{5}m$  or  $k > \frac{4}{5}m$  then
13:    Return to step 7 and choose a new grid line, executing a binary search if necessary. If this fails,
    search over horizontal grid lines  $\operatorname{Im}(z) = h$ , this time setting  $(\mathcal{A}, \mathcal{B}) = (A - i(h-1)B, A - i(h+1)B)$ .
14:  else
15:     $U_R = \mathbf{GRURV}(2, A_p + B_p, A_p, -1, 1)$ 
16:     $[A_p, B_p] = \mathbf{IRS}(A^H, B^H, p)$ 
17:     $U_L = \mathbf{GRURV}(2, A_p^H, (A_p + B_p)^H, 1, -1)$ .
18:     $U_L^H A U_R = \begin{pmatrix} A_{11} & A_{12} \\ E & A_{22} \end{pmatrix}, U_L^H B U_R = \begin{pmatrix} B_{11} & B_{12} \\ F & B_{22} \end{pmatrix} \quad \triangleright A_{11}, B_{11} \in \mathbb{C}^{k \times k}$ 
19:     $g_R = \{z \in g : \operatorname{Re}(z) > h\}$  (or  $g_R = \{z \in g : \operatorname{Im}(z) > h\}$ )
20:     $[\hat{Q}_R, \hat{Q}_L, \hat{T}_A, \hat{T}_B] = \mathbf{SCHUR}(n, A_{11}, B_{11}, \frac{4}{5}\epsilon, C, g_R, \frac{1}{\sqrt{3}}\eta, \theta)$ 
21:     $g_L = \{z \in g : \operatorname{Re}(z) < h\}$  (or  $g_L = \{z \in g : \operatorname{Im}(z) < h\}$ )
22:     $[\tilde{Q}_R, \tilde{Q}_L, \tilde{T}_A, \tilde{T}_B] = \mathbf{SCHUR}(n, A_{22}, B_{22}, \frac{4}{5}\epsilon, C, g_L, \frac{1}{\sqrt{3}}\eta, \theta)$ 
23:     $Q_R = U_R \begin{pmatrix} \hat{Q}_R & 0 \\ 0 & \tilde{Q}_R \end{pmatrix}, Q_L = U_L \begin{pmatrix} \hat{Q}_L & 0 \\ 0 & \tilde{Q}_L \end{pmatrix}$ 
24:     $T_A = \begin{pmatrix} \hat{T}_A & \hat{Q}_L^H A_{12} \tilde{Q}_R \\ 0 & \tilde{T}_A \end{pmatrix}, T_B = \begin{pmatrix} \hat{T}_B & \hat{Q}_L^H B_{12} \tilde{Q}_R \\ 0 & \tilde{T}_B \end{pmatrix}$ 
25:  end if
26: end if
27: return  $Q_R, Q_L, T_A, T_B$ 
```

for one pair of deflating subspaces instead of two. Intuitively, we can account for this by applying the guarantees of **DEFLATE** (i.e., [14, Algorithm 4]) once instead of twice. While this changes the parameters by (at most) a constant factor, we include the details for completeness.

Let $U_R = \begin{pmatrix} U_R^{(1)} & W_R \end{pmatrix}$ and $U_L = \begin{pmatrix} U_L^{(1)} & W_L \end{pmatrix}$ for $U_R^{(1)}, U_L^{(1)} \in \mathbb{C}^{m \times k}$. Taking $\nu = \sqrt{\frac{\theta}{5n^4}}$ in [14, Theorem 4.7], we are guaranteed that with probability at least $1 - \frac{2\theta}{5n^4}$ there exist $\bar{U}_R, \bar{U}_L \in \mathbb{C}^{n \times k}$ whose columns span the corresponding true right/left deflating subspaces of $(\mathcal{A}, \mathcal{B})$ and

$$\max \left\{ \|U_R^{(1)} - \bar{U}_R\|_2, \|U_L^{(1)} - \bar{U}_L\|_2 \right\} \leq \sqrt{8n^2\delta\sqrt{\frac{5k(m-k)}{\theta}}} \leq \sqrt{\sqrt{\frac{5}{\theta}}8n^3\delta}. \quad (\text{A.4})$$

The second constraint on δ therefore implies

$$\max \left\{ \|U_R^{(1)} - \bar{U}_R\|_2, \|U_L^{(1)} - \bar{U}_L\|_2 \right\} \leq \min \left\{ \frac{\epsilon}{10C}, \frac{\eta}{2\sqrt{3}C} \right\}, \quad (\text{A.5})$$

again with probability at least $1 - \frac{2\theta}{5n^4}$. As we will see, these bounds guarantee, respectively, that shattering is preserved as we recur and moreover that the error in the resulting factorization can be controlled. A simple union bound implies that at any step of the recursive procedure a good dividing line is found, k is computed correctly, and (A.5) holds with probability at least $1 - \frac{\theta}{2n^4}$.

Before moving on, we pause to consider how bounds like $\|U_R^{(1)} - \bar{U}_R\|_2 \leq \mu$ and $\|U_L^{(1)} - \bar{U}_L\|_2 \leq \mu$ can be extended to cover $\|E\|_2$ and $\|F\|_2$ in line 18. The heuristic here is fairly straightforward: if the deflating subspaces are approximated accurately enough, E and F should be nearly zero. With this in mind, let $U_R^{(1)} = \bar{U}_R + \Delta_1$ for some $\Delta_1 \in \mathbb{C}^{m \times k}$ with $\|\Delta_1\|_2 \leq \mu$. In this case,

$$E = W_L^H A U_R^{(1)} = W_L^H A (\bar{U}_R + \Delta_1) = W_L^H A \bar{U}_R + W_L^H A \Delta_1. \quad (\text{A.6})$$

Now \bar{U}_R contains a basis for the right deflating subspace of (A, B) corresponding to \bar{U}_L , so $A \bar{U}_R = \bar{U}_L X$ for some $X \in \mathbb{C}^{k \times k}$. Applying this to (A.6) and further letting $\bar{U}_L = U_L^{(1)} + \Delta_2$ for another $\Delta_2 \in \mathbb{C}^{m \times k}$ satisfying $\|\Delta_2\|_2 \leq \mu$, we have

$$E = W_L^H \bar{U}_L X + W_L^H A \Delta_1 = W_L^H (U_L^{(1)} + \Delta_2) X + W_L^H A \Delta_1 = W_L^H \Delta_2 X + W_L^H A \Delta_1, \quad (\text{A.7})$$

where the last equality follows from $W_L^H U_L^{(1)} = 0$. Hence, we conclude

$$\|E\|_2 \leq \|W_L^H \Delta_2 X\|_2 + \|W_L^H A \Delta_1\|_2 \leq \mu(\|X\|_2 + \|A\|_2). \quad (\text{A.8})$$

We can remove $\|X\|_2$ from this bound by noting $X = \bar{U}_L^H A \bar{U}_R$ and therefore $\|X\|_2 \leq \|A\|_2$. Thus, $\|E\|_2 \leq 2\mu\|A\|_2$. A similar argument yields $\|F\|_2 \leq 2\mu\|B\|_2$.

We now show that the first bound in (A.5) implies that the recursive calls in lines 20 and 22 are valid, meaning the inputs satisfy the listed requirements. Since multiplying by blocks of unitary matrices cannot violate the norm constraints, this reduces to showing that $\Lambda_{4\epsilon/5}(A_{11}, B_{11})$ and $\Lambda_{4\epsilon/5}(A_{22}, B_{22})$ are shattered with respect to g_R and g_L , respectively. For (A_{11}, B_{11}) we can simply repeat the argument used in the proof of [14, Theorem 4.8]; that is, $\|A_{11} - \bar{U}_L^H A \bar{U}_R\|_2$ and $\|B_{11} - \bar{U}_L^H B \bar{U}_R\|_2$ can both be bounded by $\frac{\epsilon}{5}$, in which case $\Lambda_{4\epsilon/5}(A_{11}, B_{11})$ is shattered with respect to g with each eigenvalue of (A_{11}, B_{11}) sharing a unique grid box with an eigenvalue of $(\bar{U}_L^H A \bar{U}_R, \bar{U}_L^H B \bar{U}_R)$. Hence, we also know that $\Lambda(A_{11}, B_{11}) \subset g_R$.

Unfortunately, the same approach cannot be used for (A_{22}, B_{22}) , as the columns of W_L and W_R do *not* approximately span deflating subspaces in general. Instead, we'll need to establish the following two items separately:

1. $\Lambda_{4\epsilon/5}(A_{22}, B_{22})$ is shattered with respect to g .
2. (A_{22}, B_{22}) has all of its eigenvalues in g_L .

We'll tackle shattering first. Suppose $z \in \Lambda_{4\epsilon/5}(A_{22}, B_{22})$. In this case, $\sigma_{m-k}(A_{22} - zB_{22}) \leq \frac{4}{5}\epsilon(1 + |z|)$ (see e.g., [20]). Since $A_{22} - zB_{22}$ is the lower right $(m-k) \times (m-k)$ block of $U_L^H AU_R - zU_L^H BU_R$, where U_L and U_R are unitary, it is easy to see that

$$\sigma_m(A - zB) = \sigma_m(U_L^H AU_R - zU_L^H BU_R) \leq \sqrt{\sigma_{m-k}(A_{22} - zB_{22})^2 + \|E - zF\|_2^2}. \quad (\text{A.9})$$

Extending (A.5) as outlined above, recalling $\|A\|_2, \|B\|_2 \leq C$, we can bound $\|E - zF\|_2$ as follows:

$$\|E - zF\|_2 \leq \|E\|_2 + |z|\|F\|_2 \leq \frac{\epsilon}{5}(1 + |z|). \quad (\text{A.10})$$

Applying this to (A.9) alongside our bound for $\sigma_{m-k}(A_{22} - zB_{22})$ yields

$$\sigma_m(A - zB) \leq \sqrt{\frac{17}{25}\epsilon(1 + |z|)} \leq \epsilon(1 + |z|), \quad (\text{A.11})$$

which implies $z \in \Lambda_\epsilon(A, B)$. Thus, $\Lambda_{4\epsilon/5}(A_{22}, B_{22}) \subseteq \Lambda_\epsilon(A, B)$; since the latter is assumed to be shattered with respect to g on input, this proves shattering for $\Lambda_{4\epsilon/5}(A_{22}, B_{22})$.

It remains to show that the eigenvalues of (A_{22}, B_{22}) lie in g_L . To do this, consider the $m \times m$ matrices

$$M_1 = \begin{pmatrix} A_{11} & A_{12} \\ 0 & A_{22} \end{pmatrix}, \quad M_2 = \begin{pmatrix} B_{11} & B_{12} \\ 0 & B_{22} \end{pmatrix}, \quad (\text{A.12})$$

which are obtained from $U_L^H AU_R$ and $U_L^H BU_R$, respectively, by zeroing out E and F . Since (M_1, M_2) is block upper triangular, its spectrum is $\Lambda(A_{11}, B_{11}) \cup \Lambda(A_{22}, B_{22})$. Moreover, we have

$$U_L^H AU_R - M_1 = \begin{pmatrix} 0 & 0 \\ E & 0 \end{pmatrix} \implies \|U_L^H AU_R - M_1\|_2 \leq \|E\|_2 \leq \frac{\epsilon}{5} \quad (\text{A.13})$$

and similarly $\|U_L^H BU_R - M_2\|_2 \leq \frac{\epsilon}{5}$. Now $\Lambda_\epsilon(U_L^H AU_R, U_L^H BU_R)$ is shattered with respect to g , so by [14, Lemma 3.14] we know that each eigenvalue of (M_1, M_2) shares a grid box with an eigenvalue of $(U_L^H AU_R, U_L^H BU_R)$.²¹ But $\Lambda(U_L^H AU_R, U_L^H BU_R) = \Lambda(A, B)$ and (A, B) has exactly k eigenvalues in g_R and $m - k$ in g_L (recall that we are assuming k has been computed accurately in line 11). Since $\Lambda(M_1, M_2) = \Lambda(A_{11}, B_{11}) \cup \Lambda(A_{22}, B_{22})$ and we showed above that (A_{11}, B_{11}) has all of its eigenvalues in g_R , this implies that (A_{22}, B_{22}) must have all of its eigenvalues in g_L .

Combining points one and two above, we conclude that $\Lambda_{4\epsilon/5}(A_{22}, B_{22})$ is shattered with respect to g_L and therefore that the call to **SCHUR** in line 22 is valid. As a result, we have proved success for one step of the recursive procedure under the conditions that (1) a good dividing line is found, (2) the corresponding value of k is accurate, and (3) the upper bound (A.5) holds. Since these occur simultaneously (at any step) with probability at least $1 - \frac{\theta}{2n^4}$, and moreover the recursive tree of **SCHUR** has depth at most $\log_{5/4}(n)$, the algorithm fails to converge with probability at most $2 \cdot 2^{\log_{5/4}(n)} \frac{\theta}{2n^4} \leq \theta$.

To complete the proof, we derive the error bounds $\|A - Q_L T_A Q_R^H\|_2 \leq \eta$ and $\|B - Q_L T_B Q_R^H\|_2 \leq \eta$ under the same assumptions. We do this inductively. The base case is $m = 1$, in which case the decomposition produced by **SCHUR** is exact. Consider now any other step of the procedure. We have

$$\begin{aligned} \|A - Q_L T_A Q_R^H\|_2 &= \|U_L^H AU_R - U_L^H Q_L T_A Q_R^H U_R\|_2 \\ &= \left\| \begin{pmatrix} A_{11} & A_{12} \\ E & A_{22} \end{pmatrix} - \begin{pmatrix} \hat{Q}_L & 0 \\ 0 & \tilde{Q}_L \end{pmatrix} \begin{pmatrix} \hat{T}_A & \hat{Q}_L^H A_{12} \tilde{Q}_R \\ 0 & \tilde{T}_A \end{pmatrix} \begin{pmatrix} \hat{Q}_R^H & 0 \\ 0 & \tilde{Q}_R^H \end{pmatrix} \right\|_2 \\ &= \left\| \begin{pmatrix} A_{11} - \hat{Q}_L \hat{T}_A \hat{Q}_R^H & 0 \\ E & A_{22} - \tilde{Q}_L \tilde{T}_A \tilde{Q}_R^H \end{pmatrix} \right\|_2 \\ &\leq \left(\|A_{11} - \hat{Q}_L \hat{T}_A \hat{Q}_R^H\|_2^2 + \|A_{22} - \tilde{Q}_L \tilde{T}_A \tilde{Q}_R^H\|_2^2 + \|E\|_2^2 \right)^{1/2}. \end{aligned} \quad (\text{A.14})$$

²¹This again follows from the fact that $\Lambda_\epsilon(A, B)$ is shattered with respect to g , as shattering is both unchanged when A and B are multiplied by unitary matrices and additionally implies that (A, B) – and therefore also $(U_L^H AU_R, U_L^H BU_R)$ – is regular.

By our induction hypothesis we can assume that $\|A_{11} - \widehat{Q}_L \widehat{T}_A \widehat{Q}_R^H\|_2$ and $\|A_{22} - \widetilde{Q}_L \widetilde{T}_A \widetilde{Q}_R\|_2$ are both bounded by $\frac{\eta}{\sqrt{3}}$. Since the second piece of (A.5) implies the same bound for $\|E\|_2$, we therefore conclude

$$\|A - Q_L T_A Q_R^H\|_2 \leq \sqrt{\left(\frac{\eta}{\sqrt{3}}\right)^2 + \left(\frac{\eta}{\sqrt{3}}\right)^2 + \left(\frac{\eta}{\sqrt{3}}\right)^2} = \eta. \quad (\text{A.15})$$

Repeating this argument yields the corresponding bound $\|B - Q_L T_B Q_R^H\|_2 \leq \eta$. \square

As a corollary, we obtain an algorithm that can compute an accurate Schur decomposition of any pencil in nearly matrix multiplication time (with high probability). Once again, note that – like all of the methods considered in this paper – this algorithm is entirely inverse-free.

Corollary A.2. *Let $(A, B) \in \mathbb{C}^{n \times n} \times \mathbb{C}^{n \times n}$ be any pencil with $\|A\|_2, \|B\|_2 \leq 1$ and let $\varepsilon < 1$. There exists an exact-arithmetic, randomized algorithm that takes as inputs (A, B) and ε and – in $O(\log^2(\frac{n}{\varepsilon})T_{\text{MM}}(n))$ operations – produces $Q_R, Q_L, T_A, T_B \in \mathbb{C}^{n \times n}$ such that Q_R and Q_L are unitary, T_A and T_B are upper triangular, and*

$$\|A - Q_L T_A Q_R^H\|_2 \leq \varepsilon \quad \text{and} \quad \|B - Q_L T_B Q_R^H\|_2 \leq \varepsilon$$

with probability at least $1 - O(\frac{1}{n})$.

Proof. Consider the following algorithm, whose only inputs are (A, B) and ε .

1. Set parameters: $\gamma = \frac{\varepsilon}{8}$; $\alpha = \frac{\lceil 2 \log_n(1/\gamma) + 3 \rceil}{2}$; $\epsilon = \frac{\gamma^5}{64n^{\frac{11\alpha+25}{3} + \gamma^5}}$; $\omega = \frac{\gamma^4}{4} n^{-\frac{8\alpha+13}{3}}$.
2. Draw two independent Ginibre matrices $G_1, G_2 \in \mathbb{C}^{n \times n}$ and let $(\widetilde{A}, \widetilde{B}) = (A + \gamma G_1, B + \gamma G_2)$.
3. Draw z uniformly at random from the box of side length ω with bottom left corner $-4 - 4i$ and let $g = \text{grid}(z, \omega, \lceil 8/\omega \rceil, \lceil 8/\omega \rceil)$.
4. $[Q_R, Q_L, T_A, T_B] = \mathbf{SCHUR}(n, \widetilde{A}, n^\alpha \widetilde{B}, \epsilon, 3n^\alpha, g, \frac{\varepsilon}{2}, \frac{1}{n})$.
5. Re-scale: $T_B = n^{-\alpha} T_B$.
6. Output Q_R, Q_L, T_A and T_B .

For the listed values of α , ϵ , and ω , [14, Theorem 3.12] guarantees that $\|\widetilde{A}\|_2 \leq 3$, $\|n^\alpha \widetilde{B}\|_2 \leq 3n^\alpha$, and $\Lambda_\epsilon(\widetilde{A}, n^\alpha \widetilde{B})$ is shattered with respect to g with probability at least $1 - O(\frac{1}{n})$. In this case the call to **SCHUR** is valid, and moreover (by Theorem A.1) it succeeds with probability at least $1 - \frac{1}{n}$, achieving

$$\|\widetilde{A} - Q_L T_A Q_R^H\|_2 \leq \frac{\varepsilon}{2} \quad \text{and} \quad \|n^\alpha \widetilde{B} - Q_L T_B Q_R^H\|_2 \leq \frac{\varepsilon}{2} \quad (\text{A.16})$$

on exit (i.e., before re-scaling T_B). Consequently,

$$\|A - Q_L T_A Q_R^H\|_2 \leq \|A - \widetilde{A}\|_2 + \|\widetilde{A} - Q_L T_A Q_R^H\|_2 \leq \frac{\varepsilon}{2} + \frac{\varepsilon}{2} \leq \varepsilon \quad (\text{A.17})$$

and similarly, again for the initial T_B ,

$$\|B - Q_L (n^{-\alpha} T_B) Q_R^H\|_2 \leq \|B - \widetilde{B}\|_2 + \|\widetilde{B} - Q_L (n^{-\alpha} T_B) Q_R^H\|_2 \leq \frac{\varepsilon}{2} + \frac{\varepsilon}{2n^\alpha} = \varepsilon. \quad (\text{A.18})$$

Here, we make use of the fact that $\|A - \widetilde{A}\|_2 = \gamma \|G_1\|_2$ and $\|B - \widetilde{B}\|_2 = \gamma \|G_2\|_2$, where we can assume $\|G_1\|_2, \|G_2\|_2 \leq 4$.²² Hence, a final union bound implies that **SCHUR** succeeds, and we achieve the desired accuracy, with probability at least $1 - O(\frac{1}{n})$. Since this algorithm does less work than its diagonalization counterpart, the complexity $O(\log^2(\frac{n}{\varepsilon})T_{\text{MM}}(n))$ follows from [14, Proposition 5.3]. \square

²²The probability that one of $\|G\|_1$ and $\|G\|_2$ is larger than four is included in the failure probability of shattering.

In the proof of [Corollary A.2](#), **SCHUR** is applied to a pencil (A, B) where A and B are minimally well-conditioned with high probability. For such inputs, we can simplify [Algorithm 5](#) by replacing lines 16 and 17 with one of the following:

$$[U_L, R] = \mathbf{QR}(BU_R) \quad \text{or} \quad [U_L, R] = \mathbf{QR}(AU_R). \quad (\text{A.19})$$

In other words, we can leverage the fact that A and B map right deflating subspaces to the corresponding left ones, trading an expensive call to **IRS** for a simple QR factorization. This results in significant savings, as QR can be done in matrix multiplication time while **IRS** requires $O(\log(\frac{n}{\varepsilon})T_{\text{MM}}(n))$ operations for the parameters chosen in the proof of [Corollary A.2](#). Moreover, when a bound on $\kappa_2(B)$ or $\kappa_2(A)$ is available, we can easily describe how error in U_R propagates to U_L . We provide a sketch for $[U_L, R] = \mathbf{QR}(BU_R)$ below.

As in the proof of [Theorem A.1](#), let $U_R = \begin{pmatrix} U_R^{(1)} & W_R \end{pmatrix}$ and $U_L = \begin{pmatrix} U_L^{(1)} & W_L \end{pmatrix}$ for $U_R^{(1)}, U_L^{(1)} \in \mathbb{C}^{m \times k}$ and suppose that $U_R^{(1)}$ has been computed to some accuracy μ – i.e., there exists a true $\bar{U}_R \in \mathbb{C}^{m \times k}$ (whose columns span the associated true right deflating subspace) such that $\|U_R^{(1)} - \bar{U}_R\|_2 \leq \mu$. Further let R_{11} be the upper left $k \times k$ block of R . In this case, $BU_R^{(1)} = U_L^{(1)}R_{11}$ and $\|BU_R^{(1)} - \bar{U}_R\|_2 \leq \mu\|B\|_2$. Hence, classical perturbation theory for reduced QR (e.g., [43]) implies that for μ sufficiently small there exists a (unique) reduced QR factorization

$$B\bar{U}_R = \bar{U}_L(R_{11} + \Delta R) \quad (\text{A.20})$$

such that²³

$$\|U_L^{(1)} - \bar{U}_L\|_2 \leq O(\sqrt{k}) \cdot \kappa_2(BU_R^{(1)}) \cdot \frac{\mu\|B\|_2}{\|BU_R^{(1)}\|_2} \leq O(\sqrt{k})\kappa_2(B)\mu \quad (\text{A.21})$$

Clearly, the columns of \bar{U}_L span the left deflating subspace corresponding to \bar{U}_R . Thus, we can simply divide μ by $O(\sqrt{k})\kappa_2(B)$ to obtain a similar accuracy guarantee for the left deflating subspace. In terms of the parameters of **SCHUR**, this would correspond to a slightly more restrictive choice of δ in line 5.

Of course, this requires a bound on $\kappa_2(B)$ (or similarly $\kappa_2(A)$). While a guarantee of pseudospectral shattering does imply that B is nonsingular, it does not necessarily guarantee that B is particularly well-conditioned; if it is not, obtaining U_L from U_R may actually be more costly than repeating **IRS** and **GRURV**. In an effort to further maintain the generality of [Algorithm 5](#), we therefore compute U_L via **IRS**. Nevertheless, [\(A.19\)](#) is likely to be the cheaper option in practice.

Remark A.3. While the parameters chosen in [Algorithm 5](#) and the proof of [Corollary A.2](#) seem restrictive, they are in fact much nicer than the diagonalization case, as we might expect. Compare in particular the dependence of δ on η in **SCHUR** versus β in **EIG**. Since most of the work in both algorithms is spent locating good dividing lines, this is the real advantage – in terms of efficiency – of going to Schur form instead of complete diagonalization. Note that recent work of Shah [37] opens the possibility of further relaxing parameters in both algorithms, though not enough to change their final asymptotic complexities.

B Proof of Theorem 2.7

In this appendix, we provide a full proof of [Theorem 2.7](#).

B.1 Technical Lemmas

We begin by stating a handful of technical lemmas. The first two are straightforward consequences of the black-box, finite-precision assumptions from [Section 2](#). Here, $\mathbf{MM}(\cdot)$ and $\mathbf{QR}(\cdot)$ are again the floating-point algorithms covered by [Assumption 2.5](#) and [Assumption 2.6](#), respectively.

Lemma B.1. *Let $A, B \in \mathbb{C}^{n \times n}$. If C is the floating-point sum of A and B then*

$$\|C - (A + B)\|_2 \leq \sqrt{n}\mathbf{u}\|A + B\|_2.$$

²³The \sqrt{k} dependence here can actually be improved to $\log(k)$ [36, Chapter 3].

Lemma B.2. Let $[Q, R] = \mathbf{QR}(A)$ for

$$A = \begin{pmatrix} A_1 \\ A_2 \end{pmatrix}, \quad Q = \begin{pmatrix} Q_{11} & Q_{12} \\ Q_{21} & Q_{22} \end{pmatrix}, \quad \text{and} \quad R = \begin{pmatrix} R' \\ 0 \end{pmatrix},$$

where all blocks are $n \times n$. Define the following matrices:

1. \tilde{R} – the floating-point sum of $\mathbf{MM}(Q_{11}^H, A_1)$ and $\mathbf{MM}(Q_{21}^H, A_2)$.
2. E – the floating-point sum of $\mathbf{MM}(Q_{12}^H, A_1)$ and $\mathbf{MM}(Q_{22}^H, A_2)$.

If $\mu_{\mathbf{QR}}(n)\mathbf{u}, \mu_{\mathbf{MM}}(n)\mathbf{u} \leq 1$, then

$$\|\tilde{R} - R\|_2, \|E\|_2 \leq 4(\mu_{\mathbf{QR}}(n) + \mu_{\mathbf{MM}}(n) + 2\sqrt{n})\mathbf{u}\|A\|_2.$$

Proof. By [Assumption 2.6](#), there exist matrices $\hat{A} \in \mathbb{C}^{2n \times n}$ and $\hat{Q} \in \mathbb{C}^{2n \times 2n}$ such that \hat{Q} is truly unitary, $\hat{A} = \hat{Q}R$, $\|Q - \hat{Q}\|_2 \leq \mu_{\mathbf{QR}}(n)\mathbf{u}$, and $\|A - \hat{A}\|_2 \leq \mu_{\mathbf{QR}}(n)\mathbf{u}\|A\|_2$. Let

$$\hat{A} = \begin{pmatrix} \hat{A}_1 \\ \hat{A}_2 \end{pmatrix} \quad \text{and} \quad \hat{Q} = \begin{pmatrix} \hat{Q}_{11} & \hat{Q}_{12} \\ \hat{Q}_{21} & \hat{Q}_{22} \end{pmatrix}, \quad (\text{B.1})$$

where again all blocks are $n \times n$. Consider first $\mathbf{MM}(Q_{11}^H, A_1)$. Applying [Assumption 2.5](#) we observe

$$\begin{aligned} \|\mathbf{MM}(Q_{11}^H, A_1) - \hat{Q}_{11}^H \hat{A}_1\|_2 &\leq \|\mathbf{MM}(Q_{11}^H, A_1) - Q_{11}^H A_1\|_2 + \|Q_{11}^H A_1 - \hat{Q}_{11}^H \hat{A}_1\|_2 \\ &\leq \mu_{\mathbf{MM}}(n)\mathbf{u}\|Q_{11}\|_2\|A_1\|_2 + \|Q_{11}^H A_1 - \hat{Q}_{11}^H \hat{A}_1\|_2 + \|\hat{Q}_{11}^H \hat{A}_1 - \hat{Q}_{11}^H \hat{A}_1\|_2 \\ &\leq \mu_{\mathbf{MM}}(n)\mathbf{u}\|Q\|_2\|A\|_2 + \|Q - \hat{Q}\|_2\|A\|_2 + \|\hat{Q}\|_2\|A - \hat{A}\|_2. \end{aligned} \quad (\text{B.2})$$

Since $\|\hat{Q}\|_2 = 1$ and therefore $\|Q\|_2 \leq \|\hat{Q}\|_2 + \mu_{\mathbf{QR}}(n)\mathbf{u} = 1 + \mu_{\mathbf{QR}}(n)\mathbf{u}$, [\(B.2\)](#) implies

$$\begin{aligned} \|\mathbf{MM}(Q_{11}^H, A_1) - \hat{Q}_{11}^H \hat{A}_1\|_2 &\leq [2\mu_{\mathbf{QR}}(n) + \mu_{\mathbf{MM}}(n)(1 + \mu_{\mathbf{QR}}(n)\mathbf{u})]\mathbf{u}\|A\|_2 \\ &\leq 2(\mu_{\mathbf{QR}}(n) + \mu_{\mathbf{MM}}(n))\mathbf{u}\|A\|_2. \end{aligned} \quad (\text{B.3})$$

Repeating this argument, swapping blocks accordingly, we obtain the same result for $\|\mathbf{MM}(Q_{21}^H, A_2) - \hat{Q}_{21}^H \hat{A}_2\|_2$, $\|\mathbf{MM}(Q_{12}^H, A_1) - \hat{Q}_{12}^H \hat{A}_1\|_2$, and $\|\mathbf{MM}(Q_{22}^H, A_2) - \hat{Q}_{22}^H \hat{A}_2\|_2$. To now bound $\|\tilde{R} - R'\|_2$, note that

$$R' = \hat{Q}_{11}^H \hat{A}_1 + \hat{Q}_{21}^H \hat{A}_2 \quad (\text{B.4})$$

since $\hat{A} = \hat{Q}R$. Consequently,

$$\begin{aligned} \|\tilde{R} - R'\|_2 &\leq \|\tilde{R} - (\mathbf{MM}(Q_{11}^H, A_1) + \mathbf{MM}(Q_{21}^H, A_2))\|_2 \\ &\quad + \|\mathbf{MM}(Q_{11}^H, A_1) - \hat{Q}_{11}^H \hat{A}_1\|_2 + \|\mathbf{MM}(Q_{21}^H, A_2) - \hat{Q}_{21}^H \hat{A}_2\|_2. \end{aligned} \quad (\text{B.5})$$

By [Lemma B.1](#), we can bound the first term by $\sqrt{n}\mathbf{u}\|\mathbf{MM}(Q_{11}^H, A_1) + \mathbf{MM}(Q_{21}^H, A_2)\|_2$, where

$$\begin{aligned} \|\mathbf{MM}(Q_{11}^H, A_1) + \mathbf{MM}(Q_{21}^H, A_2)\|_2 &\leq \|\mathbf{MM}(Q_{11}^H, A_1)\|_2 + \|\mathbf{MM}(Q_{21}^H, A_2)\|_2 \\ &\leq \|Q_{11}^H A_1\|_2 + \mu_{\mathbf{MM}}(n)\mathbf{u}\|Q_{11}\|_2\|A_1\|_2 \\ &\quad + \|Q_{21}^H A_2\|_2 + \mu_{\mathbf{MM}}(n)\mathbf{u}\|Q_{21}\|_2\|A_2\|_2 \\ &\leq 2(1 + \mu_{\mathbf{MM}}(n)\mathbf{u})(1 + \mu_{\mathbf{QR}}(n)\mathbf{u})\|A\|_2 \\ &\leq 8\|A\|_2. \end{aligned} \quad (\text{B.6})$$

Applying this to [\(B.5\)](#) alongside [\(B.3\)](#) yields

$$\|\tilde{R} - R'\|_2 \leq 4(\mu_{\mathbf{QR}}(n) + \mu_{\mathbf{MM}}(n) + 2\sqrt{n})\mathbf{u}\|A\|_2. \quad (\text{B.7})$$

We obtain the same bound for $\|E\|_2$ by repeating this argument with $\mathbf{MM}(Q_{12}^H, A_1)$ and $\mathbf{MM}(Q_{22}^H, A_2)$ and noting that $\hat{Q}_{12}^H \hat{A}_1 + \hat{Q}_{22}^H \hat{A}_2 = 0$. \square

Next, we state a pair of lemmas due to Malyshev [27, Lemmas 4.1 and 4.2].

Lemma B.3 (Malyshev 1992). *Suppose $R \in \mathbb{C}^{m \times m}$ is nonsingular and $E \in \mathbb{C}^{n \times m}$ for $m \geq n$. There exists a matrix $S \in \mathbb{C}^{(m+n) \times (m+n)}$ such that*

1. $(I + S) \begin{pmatrix} R \\ E \end{pmatrix} = \begin{pmatrix} R' \\ 0 \end{pmatrix}$.
2. $(I + S)^H (I + S) = I$
3. $\|S\|_2 \leq \|ER^{-1}\|_2 \leq \|E\|_2 \|R^{-1}\|_2$.

Proof. We take the opportunity to correct a small error in Malyshev’s proof. Define

$$\tilde{S} = \begin{pmatrix} 0 & (ER^{-1})^H \\ -ER^{-1} & 0 \end{pmatrix}. \quad (\text{B.8})$$

Then the matrix

$$S = \begin{pmatrix} [I + (ER^{-1})^H ER^{-1}]^{-1/2} & 0 \\ 0 & [I + ER^{-1}(ER^{-1})^H]^{-1/2} \end{pmatrix} (I + \tilde{S}) - I \quad (\text{B.9})$$

satisfies the listed requirements. \square

Lemma B.4 (Malyshev 1992). *Let $A \in \mathbb{C}^{m \times n}$ be full rank and suppose*

$$A = Q_1 \begin{pmatrix} K_1 & L_1 \\ 0 & M_1 \end{pmatrix} = Q_2 \begin{pmatrix} K_2 & L_2 \\ 0 & M_2 \end{pmatrix}$$

for $Q_1, Q_2 \in \mathbb{C}^{m \times m}$ unitary, $K_1, K_2 \in \mathbb{C}^{k \times k}$ nonsingular, and $M_1, M_2 \in \mathbb{C}^{(m-k) \times (n-k)}$ full rank. Then there exist unitary matrices $P \in \mathbb{C}^{k \times k}$ and $Q \in \mathbb{C}^{(n-k) \times (n-k)}$ such that $K_2 = PK_1$, $L_2 = PL_1$, and $M_2 = QM_1$.

B.2 Detailed Proof

We are now ready to bound error in **IRS**. To simplify the analysis, we will not track the individual polynomials $\mu_{\text{MM}}(n)$ and $\mu_{\text{QR}}(n)$, instead working with a “general polynomial”

$$\mu(n) = \max \{ \mu_{\text{MM}}(n), \mu_{\text{QR}}(n), \sqrt{n} \} \quad (\text{B.10})$$

and the associated quantity $\tau = \mu(n)\mathbf{u}$. Throughout, we can think of τ as small, corresponding to a choice $\mathbf{u} < \mu(n)^{-1}$.

Before proceeding with our main argument we state one final lemma, which bounds norm growth in repeated squaring. Because finite-precision **IRS** repeatedly multiplies the inputs by pieces of nearly unitary matrices, we expect that norms should grow by (at most) small constants. Here, \tilde{A}_j and \tilde{B}_j are the outputs of j steps of finite-precision **IRS**, beginning with the input matrices $\tilde{A}_0 = A$ and $\tilde{B}_0 = B$.

Lemma B.5. *At any step j , $\| \begin{pmatrix} \tilde{A}_{j+1} \\ \tilde{B}_{j+1} \end{pmatrix} \|_2 \leq (1 + 2\tau)^2 \| \begin{pmatrix} \tilde{A}_j \\ \tilde{B}_j \end{pmatrix} \|_2$.*

Proof. Recall that $\tilde{A}_{j+1} = \text{MM}(\tilde{Q}_{12}^H, \tilde{A}_j)$ and $\tilde{B}_{j+1} = \text{MM}(\tilde{Q}_{22}^H, \tilde{B}_j)$ for \tilde{Q}_{12} and \tilde{Q}_{22} blocks of a nearly unitary \tilde{Q} obtained by computing a finite-precision, full QR factorization of $\begin{pmatrix} \tilde{B}_j \\ -\tilde{A}_j \end{pmatrix}$. With this in mind, write

$$\left\| \begin{pmatrix} \tilde{A}_{j+1} \\ \tilde{B}_{j+1} \end{pmatrix} \right\|_2 \leq \left\| \begin{pmatrix} \tilde{A}_{j+1} - \tilde{Q}_{12}^H \tilde{A}_j \\ \tilde{B}_{j+1} - \tilde{Q}_{22}^H \tilde{B}_j \end{pmatrix} \right\|_2 + \left\| \begin{pmatrix} \tilde{Q}_{12}^H \tilde{A}_j \\ \tilde{Q}_{22}^H \tilde{B}_j \end{pmatrix} \right\|_2. \quad (\text{B.11})$$

By [Assumption 2.5](#), $\| \tilde{A}_{j+1} - \tilde{Q}_{12}^H \tilde{A}_j \|_2 \leq \tau \| \tilde{Q}_{12} \|_2 \| \tilde{A}_j \|_2$ and $\| \tilde{B}_{j+1} - \tilde{Q}_{22}^H \tilde{B}_j \|_2 \leq \tau \| \tilde{Q}_{22} \|_2 \| \tilde{B}_j \|_2$, so

$$\left\| \begin{pmatrix} \tilde{A}_{j+1} - \tilde{Q}_{12}^H \tilde{A}_j \\ \tilde{B}_{j+1} - \tilde{Q}_{22}^H \tilde{B}_j \end{pmatrix} \right\|_2 \leq \sqrt{2}\tau(1 + \tau) \left\| \begin{pmatrix} \tilde{A}_j \\ \tilde{B}_j \end{pmatrix} \right\|_2 \quad (\text{B.12})$$

since \tilde{Q}_{12} and \tilde{Q}_{22} satisfy $\|\tilde{Q}_{12}\|_2, \|\tilde{Q}_{22}\|_2 \leq \|\tilde{Q}\|_2 \leq 1 + \tau$ and $\|\tilde{A}_j\|_2, \|\tilde{B}_j\|_2 \leq \|(\tilde{A}_j / \tilde{B}_j)\|_2$. Similarly,

$$\left\| \begin{pmatrix} \tilde{Q}_{12}^H \tilde{A}_j \\ \tilde{Q}_{22}^H \tilde{B}_j \end{pmatrix} \right\|_2 \leq \left\| \begin{pmatrix} \tilde{Q}_{12}^H & 0 \\ 0 & \tilde{Q}_{22}^H \end{pmatrix} \right\|_2 \left\| \begin{pmatrix} \tilde{A}_j \\ \tilde{B}_j \end{pmatrix} \right\|_2 \leq (1 + \tau) \left\| \begin{pmatrix} \tilde{A}_j \\ \tilde{B}_j \end{pmatrix} \right\|_2. \quad (\text{B.13})$$

We obtain the final inequality by combining (B.12) and (B.13) and using the loose²⁴ upper bound $(\sqrt{2}\tau + 1)(1 + \tau) \leq (1 + 2\tau)^2$. \square

We now derive the main bound of [Theorem 2.7](#). The high-level strategy of its proof, which again is due to Malyshev [27], can be summarized as follows. Consider the $2^p n \times (2^p + 1)n$ block matrix

$$M = \begin{pmatrix} -A & B & & & \\ & -A & B & & \\ & & \ddots & \ddots & \\ & & & -A & B \end{pmatrix}. \quad (\text{B.14})$$

As we demonstrate below, the floating-point matrices used to obtain \tilde{A}_p and \tilde{B}_p via **IRS** can be built into an approximate block QR factorization of M (containing \tilde{A}_p and \tilde{B}_p). Our goal will be to derive a nearby, *exact* block QR factorization of M , which will contain exact outputs \hat{A}_p and \hat{B}_p with bounds on $\|\tilde{A}_p - \hat{A}_p\|_2$ and $\|\tilde{B}_p - \hat{B}_p\|_2$ available. Since it will be relevant later on, note that the middle $2^p n \times (2^p - 1)n$ block of M is the matrix $D_{(A,B)}^p$ from [Definition 2.3](#).

To improve readability, we break this proof into several steps, each of which is labeled in bold.

Step One: What happens if we apply the output of IRS to M in blocks?

Consider the first iteration of **IRS**, which computes

$$\left[\tilde{Q}_1, \begin{pmatrix} R_1 \\ 0 \end{pmatrix} \right] = \mathbf{QR} \left(\begin{bmatrix} B \\ -A \end{bmatrix} \right) \quad (\text{B.15})$$

for nearly unitary $\tilde{Q}_1 \in \mathbb{C}^{2n \times 2n}$ and upper triangular $R_1 \in \mathbb{C}^{n \times n}$. Let \tilde{P}_1 be the matrix

$$\tilde{P}_1 = \begin{pmatrix} \tilde{Q}_1 & & \\ & \ddots & \\ & & \tilde{Q}_1 \end{pmatrix} \in \mathbb{C}^{2^p n \times 2^p n} \quad (\text{B.16})$$

containing 2^{p-1} copies of \tilde{Q}_1 on its diagonal. Further, let \tilde{M}_1 be a floating-point approximation of $\tilde{P}_1^H M$ obtained by applying **MM** (and finite-precision matrix addition) in $n \times n$ blocks. It is easy to see that \tilde{M}_1 has block structure

$$\tilde{M}_1 = \begin{pmatrix} * & \tilde{R}_1 & * & & & & \\ -\tilde{A}_1 & \tilde{E}_1 & \tilde{B}_1 & & & & \\ & & * & \tilde{R}_1 & * & & \\ & & -\tilde{A}_1 & \tilde{E}_1 & \tilde{B}_1 & & \\ & & & & \ddots & \ddots & \\ & & & & & * & \tilde{R}_1 & * \\ & & & & & -\tilde{A}_1 & \tilde{E}_1 & \tilde{B}_1 \end{pmatrix}, \quad (\text{B.17})$$

where $*$ blocks are arbitrary. We use finite-arithmetic block matrix multiplication here – as opposed to a separate black-box algorithm for large, non-square matrices – to guarantee that \tilde{A}_1 and \tilde{B}_1 appear in (B.17). Note that the zero blocks of \tilde{M}_1 are computed exactly by **MM**. Moreover, \tilde{R}_1 and \tilde{E}_1 are covered by [Lemma B.2](#) – i.e.,

$$\|\tilde{R}_1 - R_1\|_2, \|\tilde{E}_1\|_2 \leq 16\tau \left\| \begin{pmatrix} A \\ B \end{pmatrix} \right\|_2. \quad (\text{B.18})$$

²⁴We use this bound for convenience to simplify constants. As we will see, it does not significantly impact the final result.

Step Two: Repeat this argument for the next iteration.

The second step of **IRS** computes

$$\left[\tilde{U}, \begin{pmatrix} R_2 \\ 0 \end{pmatrix} \right] = \mathbf{QR} \left(\begin{bmatrix} \tilde{B}_1 \\ -\tilde{A}_1 \end{bmatrix} \right), \quad (\text{B.19})$$

for $\tilde{U} \in \mathbb{C}^{2n \times 2n}$ and $R_2 \in \mathbb{C}^{n \times n}$. Breaking \tilde{U} into $n \times n$ blocks $\tilde{U} = \begin{pmatrix} \tilde{U}_{11} & \tilde{U}_{12} \\ \tilde{U}_{21} & \tilde{U}_{22} \end{pmatrix}$ and constructing

$$\tilde{Q}_2 = \begin{pmatrix} I_n & & & \\ & \tilde{U}_{11} & & \tilde{U}_{12} \\ & & I_n & \\ & \tilde{U}_{21} & & \tilde{U}_{22} \end{pmatrix} \in \mathbb{C}^{4n \times 4n}, \quad (\text{B.20})$$

let \tilde{P}_2 be the matrix containing 2^{p-2} copies of \tilde{Q}_2 on its diagonal – that is,

$$\tilde{P}_2 = \begin{pmatrix} \tilde{Q}_2 & & \\ & \ddots & \\ & & \tilde{Q}_2 \end{pmatrix} \in \mathbb{C}^{2^p n \times 2^p n}. \quad (\text{B.21})$$

Again applying **MM** in $n \times n$ blocks to left-multiply \tilde{M}_1 by \tilde{P}_2 , we obtain \tilde{M}_2 – a finite-precision version of $\tilde{P}_2^H \tilde{M}_1$ consisting of 2^{p-2} blocks of the form

$$\begin{pmatrix} * & \tilde{R}_1 & * & & \\ * & * & \tilde{R}_2 & * & * \\ & & * & \tilde{R}_1 & * \\ -\tilde{A}_2 & \mathbf{MM}(\tilde{U}_{12}^H, \tilde{E}_1) & \tilde{E}_2 & \mathbf{MM}(\tilde{U}_{22}^H, \tilde{E}_1) & \tilde{B}_2 \end{pmatrix}. \quad (\text{B.22})$$

Step Three: Generalize to an arbitrary step of IRS.

The process outlined above yields a sequence of $2^p n \times (2^p + 1)n$ matrices $\tilde{M}_1, \dots, \tilde{M}_p$. Each \tilde{M}_i is an approximation of the exact product $\tilde{M}_i = \tilde{P}_i^H \tilde{P}_{i-1}^H \dots \tilde{P}_1^H M$ for a corresponding set of nearly unitary matrices $\tilde{P}_1, \dots, \tilde{P}_p$, each of which is constructed from the blocks of a $2n \times 2n$ nearly unitary matrix as in (B.20). Moreover, \tilde{M}_i consists of 2^{p-i} blocks with structure

$$\begin{pmatrix} * & * & * \\ -\tilde{A}_i & \tilde{\Delta}_i & \tilde{B}_i \end{pmatrix} \quad (\text{B.23})$$

for $\tilde{\Delta}_i$ a small $n \times (2^i - 1)n$ matrix. Indeed, the center $n \times n$ block \tilde{E}_i of $\tilde{\Delta}_i$ satisfies

$$\|\tilde{E}_i\|_2 \leq 16\tau \left\| \begin{pmatrix} \tilde{B}_{i-1} \\ -\tilde{A}_{i-1} \end{pmatrix} \right\|_2 \leq 16\tau(1 + 2\tau)^{2i-2} \left\| \begin{pmatrix} A \\ B \end{pmatrix} \right\|. \quad (\text{B.24})$$

Step Four: Construct a corresponding set of exact-arithmetic block matrices.

Suppose that \tilde{P}_i is constructed from the blocks of the nearly unitary matrix $\tilde{Q} \in \mathbb{C}^{2n \times 2n}$. Since we use **QR** to obtain \tilde{Q} , as described above, we know by [Assumption 2.6](#) that there exists a truly unitary matrix $Q \in \mathbb{C}^{2n \times 2n}$ such that $\|\tilde{Q} - Q\|_2 \leq \mu_{\text{QR}}(n)\mathbf{u} \leq \tau$. With this in mind, let P_i be the truly unitary matrix that has the same block structure as \tilde{P}_i but swaps the blocks of \tilde{Q} for the corresponding blocks of Q and define the $2^p n \times (2^p + 1)n$ matrices $M_i = P_i^H \dots P_1^H M$.

We now have two sets of exact-arithmetic matrices to work with: M_i and \widehat{M}_i . The former can be

thought of as an exact-arithmetic counterpart of \widetilde{M}_i while \widehat{M}_i is an intermediate matrix, obtained via exact multiplication with the nearly unitary \widetilde{P}_i . Since $\|P_i - \widetilde{P}_i\|_2 \leq \tau$ by construction, we can easily bound $\|\widehat{M}_i - M_i\|_2$ recursively:

$$\begin{aligned}
\|\widehat{M}_i - M_i\|_2 &= \|\widehat{M}_i - P_i^H \widehat{M}_{i-1} + P_i^H \widehat{M}_{i-1} - M_i\|_2 \\
&\leq \|\widehat{M}_i - P_i^H \widehat{M}_{i-1}\|_2 + \|P_i^H \widehat{M}_{i-1} - M_i\|_2 \\
&\leq \|\widetilde{P}_i - P_i\|_2 \|\widehat{M}_{i-1}\|_2 + \|P_i\|_2 \|\widehat{M}_{i-1} - M_{i-1}\|_2 \\
&\leq \tau(1 + \tau)^{i-1} \|M\|_2 + \|\widehat{M}_{i-1} - M_{i-1}\|_2
\end{aligned} \tag{B.25}$$

The base case here is $\|\widehat{M}_1 - M_1\|_2 \leq \|\widetilde{P}_1 - P_1\|_2 \|M\|_2 \leq \tau \|M\|_2$, so by induction we obtain

$$\|\widehat{M}_i - M_i\|_2 \leq \left(\sum_{j=0}^{i-1} (1 + \tau)^j \right) \tau \|M\|_2 = [(1 + \tau)^i - 1] \|M\|_2. \tag{B.26}$$

Note that \widehat{M}_i and M_i have the same block structure as \widetilde{M}_i , a consequence of the fact that each P_i has the same block structure as \widetilde{P}_i . Following (B.23), label the blocks of \widehat{M}_i and M_i as

$$\begin{pmatrix} * & * & * \\ -\widehat{A}_i & \widehat{\Delta}_i & \widehat{B}_i \end{pmatrix} \quad \text{and} \quad \begin{pmatrix} * & * & * \\ -A_i & \Delta_i & B_i \end{pmatrix}, \tag{B.27}$$

respectively, where again $*$ blocks are arbitrary and $\widehat{\Delta}_i, \Delta_i \in \mathbb{C}^{n \times (2^i - 1)n}$.

Step Five: Bound $\|\widetilde{A}_i - A_i\|_2$ and $\|\widetilde{B}_i - B_i\|_2$.

The matrices A_i and B_i in (B.27) are not necessarily the result of applying i steps of exact-arithmetic repeated squaring to A and B , as the matrices P_i used to obtain A_i and B_i from M do not correspond to true QR factorizations of exact outputs. Rather, Assumption 2.6 implies that each P_i is constructed from the Q-factor of a matrix nearby $\begin{pmatrix} B_j \\ -A_j \end{pmatrix}$. With this in mind, we next bound $\|\widetilde{A}_i - A_i\|_2$ and $\|\widetilde{B}_i - B_i\|_2$.

Consider first $\|\widetilde{A}_i - A_i\|_2$. Since

$$\|\widetilde{A}_i - A_i\|_2 \leq \|\widetilde{A}_i - \widehat{A}_i\|_2 + \|\widehat{A}_i - A_i\|_2 \leq \|\widetilde{A}_i - \widehat{A}_i\|_2 + \|\widehat{M}_i - M_i\|_2, \tag{B.28}$$

and given (B.26), we can bound $\|\widetilde{A}_i - A_i\|_2$ via (B.28) by bounding $\|\widetilde{A}_i - \widehat{A}_i\|_2$, which records the error due to finite-precision, block matrix multiplication. With this in mind, suppose $\widetilde{A}_i = \mathbf{MM}(\widetilde{Q}_{12}^H, \widetilde{A}_{i-1})$ for \widetilde{Q}_{12} an $n \times n$ block of a nearly unitary $2n \times 2n$ matrix. In this case, $\widehat{A}_i = \widetilde{Q}_{12}^H \widehat{A}_{i-1}$ and we have

$$\begin{aligned}
\|\widetilde{A}_i - \widehat{A}_i\|_2 &= \|\mathbf{MM}(\widetilde{Q}_{12}^H, \widetilde{A}_{i-1}) - \widetilde{Q}_{12}^H \widehat{A}_{i-1}\|_2 \\
&= \|\mathbf{MM}(\widetilde{Q}_{12}^H, \widetilde{A}_{i-1}) - \widetilde{Q}_{12}^H \widetilde{A}_{i-1} + \widetilde{Q}_{12}^H \widetilde{A}_{i-1} - \widetilde{Q}_{12}^H \widehat{A}_{i-1}\|_2 \\
&\leq \|\mathbf{MM}(\widetilde{Q}_{12}^H, \widetilde{A}_{i-1}) - \widetilde{Q}_{12}^H \widetilde{A}_{i-1}\|_2 + \|\widetilde{Q}_{12}^H \widetilde{A}_{i-1} - \widetilde{Q}_{12}^H \widehat{A}_{i-1}\|_2.
\end{aligned} \tag{B.29}$$

Applying our black-box assumptions and Lemma B.5, we have

$$\begin{aligned}
\|\widetilde{A}_i - \widehat{A}_i\|_2 &\leq \tau \|\widetilde{Q}_{12}\|_2 \|\widetilde{A}_{i-1}\|_2 + \|\widetilde{Q}_{12}\|_2 \|\widetilde{A}_{i-1} - \widehat{A}_{i-1}\|_2 \\
&\leq \tau(1 + \tau) \left\| \begin{pmatrix} \widetilde{A}_{i-1} \\ \widetilde{B}_{i-1} \end{pmatrix} \right\|_2 + (1 + \tau) \|\widetilde{A}_{i-1} - \widehat{A}_{i-1}\|_2 \\
&\leq \tau(1 + \tau)(1 + 2\tau)^{2i-2} \left\| \begin{pmatrix} A \\ B \end{pmatrix} \right\|_2 + (1 + \tau) \|\widetilde{A}_{i-1} - \widehat{A}_{i-1}\|_2.
\end{aligned} \tag{B.30}$$

Once again we obtain a recursive bound. In this notation $\widetilde{A}_0 = \widehat{A}_0 = A$, so the base case here is simply the

error in one finite-precision $n \times n$ matrix multiplication – i.e.,

$$\|\tilde{A}_1 - \hat{A}_1\|_2 \leq \tau(1 + \tau)\|A\|_2 \leq \tau(1 + \tau) \left\| \begin{pmatrix} A \\ B \end{pmatrix} \right\|_2. \quad (\text{B.31})$$

Thus, we conclude inductively

$$\begin{aligned} \|\tilde{A}_i - \hat{A}_i\|_2 &\leq \tau \left(\sum_{j=1}^i (1 + \tau)^{i-j+1} (1 + 2\tau)^{2j-2} \right) \left\| \begin{pmatrix} A \\ B \end{pmatrix} \right\|_2 \\ &= \tau(1 + 2\tau)^{2i} \left(\sum_{j=1}^i \left[\frac{1 + \tau}{(1 + 2\tau)^2} \right]^{i-j+1} \right) \left\| \begin{pmatrix} A \\ B \end{pmatrix} \right\|_2 \\ &= \tau(1 + 2\tau)^{2i} \cdot \frac{1 + \tau}{(1 + 2\tau)^2} \cdot \frac{1 - \left(\frac{1 + \tau}{(1 + 2\tau)^2} \right)^i}{1 - \frac{1 + \tau}{(1 + 2\tau)^2}} \cdot \left\| \begin{pmatrix} A \\ B \end{pmatrix} \right\|_2 \\ &= \frac{1 + \tau}{3 + 4\tau} [(1 + 2\tau)^{2i} - (1 + \tau)^i] \left\| \begin{pmatrix} A \\ B \end{pmatrix} \right\|_2. \end{aligned} \quad (\text{B.32})$$

Combining this with (B.26) and $\frac{1 + \tau}{3 + 4\tau} < 1$, and noting $\|M\|_2 \leq \|A\|_2 + \|B\|_2 \leq 2\left\| \begin{pmatrix} A \\ B \end{pmatrix} \right\|_2$, we have

$$\begin{aligned} \|\tilde{A}_i - A_i\|_2 &\leq [(1 + 2\tau)^{2i} - (1 + \tau)^i] \left\| \begin{pmatrix} A \\ B \end{pmatrix} \right\|_2 + 2[(1 + \tau)^i - 1] \left\| \begin{pmatrix} A \\ B \end{pmatrix} \right\|_2 \\ &= [(1 + 2\tau)^{2i} + (1 + \tau)^i - 2] \left\| \begin{pmatrix} A \\ B \end{pmatrix} \right\|_2. \end{aligned} \quad (\text{B.33})$$

Repeating this argument implies the same bound for $\|\tilde{B}_i - B_i\|_2$.

Step Six: Show that $\|\Delta_i\|_2$ is small.

If M_i was obtained from M via exact-arithmetic repeated squaring, we would have $\Delta_i = 0$. Hence, the norm of Δ_i is an indication of how far A_i and B_i are from exact outputs. With this in mind, we next derive a bound on $\|\Delta_i\|_2$.

We start by bounding $\|\hat{\Delta}_i\|_2$, beginning with its middle $n \times n$ block \hat{E}_i , which corresponds to \tilde{E}_i in \tilde{M}_i . If we again assume that \tilde{P}_i is built from the $2n \times 2n$ nearly unitary matrix $\tilde{Q} = \begin{pmatrix} \tilde{Q}_{11} & \tilde{Q}_{12} \\ \tilde{Q}_{21} & \tilde{Q}_{22} \end{pmatrix}$, we know that \tilde{E}_i is the finite-arithmetic sum of $\mathbf{MM}(\tilde{Q}_{12}^H, \tilde{B}_{i-1})$ and $\mathbf{MM}(\tilde{Q}_{22}^H, -\tilde{A}_{i-1})$ while $\hat{E}_i = \tilde{Q}_{12}^H \hat{B}_{i-1} - \tilde{Q}_{22}^H \hat{A}_{i-1}$. Hence, we have

$$\begin{aligned} \|\tilde{E}_i - \hat{E}_i\|_2 &\leq \|\tilde{E}_i - (\mathbf{MM}(\tilde{Q}_{12}^H, \tilde{B}_{i-1}) + \mathbf{MM}(\tilde{Q}_{22}^H, -\tilde{A}_{i-1}))\|_2 \\ &\quad + \|\mathbf{MM}(\tilde{Q}_{12}^H, \tilde{B}_{i-1}) - \tilde{Q}_{12}^H \hat{B}_{i-1}\|_2 + \|\mathbf{MM}(\tilde{Q}_{22}^H, \tilde{A}_{i-1}) - \tilde{Q}_{22}^H \hat{A}_{i-1}\|_2. \end{aligned} \quad (\text{B.34})$$

By [Lemma B.1](#), the first term in this expression can be bounded by

$$\begin{aligned}
& \tau \|\mathbf{MM}(\tilde{Q}_{12}^H, \tilde{B}_{i-1}) + \mathbf{MM}(\tilde{Q}_{22}^H, -\tilde{A}_{i-1})\|_2 \\
& \leq \tau \left[\|\mathbf{MM}(\tilde{Q}_{12}^H, \tilde{B}_{i-1})\|_2 + \|\mathbf{MM}(\tilde{Q}_{22}^H, -\tilde{A}_{i-1})\|_2 \right] \\
& \leq \tau \left[\|\tilde{Q}_{12}^H \tilde{B}_{i-1}\|_2 + \tau \|\tilde{Q}_{12}\|_2 \|\tilde{B}_{i-1}\|_2 + \|\tilde{Q}_{22}^H \tilde{A}_{i-1}\|_2 + \tau \|\tilde{Q}_{22}\|_2 \|\tilde{A}_{i-1}\|_2 \right] \\
& \leq \tau(1+\tau)^2 \left[\|\tilde{B}_{i-1}\|_2 + \|\tilde{A}_{i-1}\|_2 \right] \\
& \leq 2\tau(1+\tau)^2 \left\| \begin{pmatrix} \tilde{A}_{i-1} \\ \tilde{B}_{i-1} \end{pmatrix} \right\|_2 \\
& \leq 2\tau(1+\tau)^2(1+2\tau)^{2i-2} \left\| \begin{pmatrix} A \\ B \end{pmatrix} \right\|_2,
\end{aligned} \tag{B.35}$$

where the last inequality follows from [Lemma B.5](#). Using [\(B.32\)](#), the remaining terms of [\(B.34\)](#) satisfy the following:

$$\begin{aligned}
& \|\mathbf{MM}(\tilde{Q}_{22}^H, \tilde{A}_{i-1}) - \tilde{Q}_{22}^H \hat{A}_{i-1}\|_2 \\
& \leq \|\mathbf{MM}(\tilde{Q}_{22}^H, \tilde{A}_{i-1}) - \tilde{Q}_{22}^H \tilde{A}_{i-1}\|_2 + \|\tilde{Q}_{22}^H \tilde{A}_{i-1} - \tilde{Q}_{22}^H \hat{A}_{i-1}\|_2 \\
& \leq \tau \|\tilde{Q}_{22}\|_2 \|\tilde{A}_{i-1}\|_2 + \|\tilde{Q}_{22}\|_2 \|\tilde{A}_{i-1} - \hat{A}_{i-1}\|_2 \\
& \leq \tau(1+\tau) \|\tilde{A}_{i-1}\|_2 + (1+\tau) \|\tilde{A}_{i-1} - \hat{A}_{i-1}\|_2 \\
& \leq [(1+\tau)^2(1+2\tau)^{2i-2} - (1+\tau)^i] \left\| \begin{pmatrix} A \\ B \end{pmatrix} \right\|_2.
\end{aligned} \tag{B.36}$$

Putting everything together, we obtain

$$\|\tilde{E}_i - \hat{E}_i\|_2 \leq 2[(1+\tau)^3(1+2\tau)^{2i-2} - (1+\tau)^i] \left\| \begin{pmatrix} A \\ B \end{pmatrix} \right\|_2. \tag{B.37}$$

To extend this bound to all of $\hat{\Delta}_i$, note that

$$\hat{\Delta}_i = \begin{pmatrix} \tilde{Q}_{12}^H \hat{\Delta}_{i-1} & \hat{E}_i & \tilde{Q}_{22}^H \hat{\Delta}_{i-1} \end{pmatrix} \tag{B.38}$$

for the same \tilde{Q}_{12} and \tilde{Q}_{22} used above. Hence, applying both [\(B.24\)](#) and [\(B.37\)](#), we have

$$\begin{aligned}
\|\hat{\Delta}_i\|_2 & \leq \left\| \begin{bmatrix} \tilde{Q}_{12}^H \hat{\Delta}_{i-1} & \tilde{Q}_{22}^H \hat{\Delta}_{i-1} \end{bmatrix} \right\|_2 + \|\hat{E}_i\|_2 \\
& \leq \left\| \begin{bmatrix} \tilde{Q}_{12}^H & \tilde{Q}_{22}^H \end{bmatrix} \right\|_2 \|\hat{\Delta}_{i-1}\|_2 + \|\tilde{E}_i\|_2 + \|\tilde{E}_i - \hat{E}_i\|_2 \\
& \leq (1+\tau) \|\hat{\Delta}_{i-1}\|_2 + 2[(8\tau + (1+\tau)^3)(1+2\tau)^{2i-2} - (1+\tau)^i] \left\| \begin{pmatrix} A \\ B \end{pmatrix} \right\|_2 \\
& \leq (1+\tau) \|\hat{\Delta}_{i-1}\|_2 + 2[(1+15\tau)(1+2\tau)^{2i-2} - (1+\tau)^i] \left\| \begin{pmatrix} A \\ B \end{pmatrix} \right\|_2,
\end{aligned} \tag{B.39}$$

where we obtain the final inequality via $8\tau + (1+\tau)^3 \leq 1 + 15\tau$. Observing $\|\hat{\Delta}_1\|_2 = \|\hat{E}_1\|_2 \leq 28\tau \left\| \begin{pmatrix} A \\ B \end{pmatrix} \right\|_2$, [\(B.39\)](#) implies inductively

$$\|\hat{\Delta}_i\|_2 \leq 2(1+\tau)^i \left[\frac{14\tau}{1+\tau} + (1+15\tau) \sum_{j=1}^{i-1} \frac{(1+2\tau)^{2j}}{(1+\tau)^{j+1}} - (i-1) \right] \left\| \begin{pmatrix} A \\ B \end{pmatrix} \right\|_2. \tag{B.40}$$

We therefore conclude,

$$\|\hat{\Delta}_i\|_2 \leq 2(14\tau(1+\tau)^{i-1} + (i-1)[(1+15\tau)(1+2\tau)^{2i} - (1+\tau)^i]) \left\| \begin{pmatrix} A \\ B \end{pmatrix} \right\|_2, \tag{B.41}$$

which we obtain by bounding the sum in (B.40) as

$$(1 + \tau)^i \sum_{j=1}^{i-1} \frac{(1 + 2\tau)^{2j}}{(1 + \tau)^{j+1}} = \frac{(1 + 2\tau)^{2i}}{1 + \tau} \sum_{j=1}^{i-1} \left[\frac{1 + \tau}{(1 + 2\tau)^2} \right]^{i-j} \leq (i - 1)(1 + 2\tau)^{2i}, \quad (\text{B.42})$$

noting $\frac{1+\tau}{(1+2\tau)^2} < 1$. Combining (B.41) with (B.26) we have a final bound

$$\begin{aligned} \|\Delta_i\|_2 &\leq \|\widehat{\Delta}_i\|_2 + \|\widehat{\Delta}_i - \Delta_i\|_2 \\ &\leq \|\widehat{\Delta}_i\|_2 + \|\widehat{M}_i - M_i\|_2 \\ &\leq 2(14\tau(1 + \tau)^{i-1} + (i - 1)[(1 + 15\tau)(1 + 2\tau)^{2i} - (1 + \tau)^i] + (1 + \tau)^i - 1) \left\| \begin{pmatrix} A \\ B \end{pmatrix} \right\|_2. \end{aligned} \quad (\text{B.43})$$

Step Seven: Obtain $\mathring{A}_p, \mathring{B}_p$ by transforming M_p to block upper triangular.

When $i = p$, the matrix M_i consists of only one block of the form (B.27). Hence, we have shown so far

$$\widehat{P}_p^H \widehat{P}_{p-1}^H \cdots \widehat{P}_1^H M = \begin{pmatrix} * & * & * \\ -A_p & \Delta_p & B_p \end{pmatrix}, \quad (\text{B.44})$$

where each \widehat{P}_i is unitary, $\Delta_p \in \mathbb{C}^{n \times (2^p - 1)n}$ is small, and A_p and B_p are close to our finite-precision outputs \widetilde{A}_p and \widetilde{B}_p . Letting $\Pi \in \mathbb{C}^{(2^p + 1)n \times (2^p + 1)n}$ be the permutation matrix that swaps the blocks of (B.44) containing $-A_p$ and Δ_p , we have constructed an exact, almost-block-QR factorization

$$\widehat{P}_p^H \widehat{P}_{p-1}^H \cdots \widehat{P}_1^H M \Pi = \begin{pmatrix} * & * & * \\ \Delta_p & -A_p & B_p \end{pmatrix}. \quad (\text{B.45})$$

Equivalently, recalling that the middle $2^p n \times (2^p - 1)n$ block of M is $D_{(A,B)}^p$, we have found an exact factorization $\widehat{P}_p^H \cdots \widehat{P}_1^H D_{(A,B)}^p = \begin{pmatrix} * \\ \Delta_p \end{pmatrix}$.

Label the $*$ block of this matrix as $F \in \mathbb{C}^{(2^p - 1)n \times (2^p - 1)n}$. By Lemma B.3, there exists $S \in \mathbb{C}^{2^p n \times 2^p n}$ such that $I + S$ is unitary, $(I + S) \begin{pmatrix} F \\ \Delta_p \end{pmatrix} = \begin{pmatrix} F' \\ 0 \end{pmatrix}$, and

$$\|S\|_2 \leq \|\Delta_p\|_2 \|F^{-1}\|_2 \leq \frac{\|\Delta_p\|_2}{\sigma_{\min}(D_{(A,B)}^p) - \|\Delta_p\|_2}, \quad (\text{B.46})$$

assuming $\sigma_{\min}(D_{(A,B)}^p) > \|\Delta_p\|_2$. Supposing this is the case, let

$$(I + S) \widehat{P}_p^H \widehat{P}_{p-1}^H \cdots \widehat{P}_1^H M \Pi = \begin{pmatrix} * & * & * \\ 0 & -\mathring{A}_p & \mathring{B}_p \end{pmatrix} \quad (\text{B.47})$$

and note

$$\|\mathring{A}_p - A_p\|_2, \|\mathring{B}_p - B_p\|_2 \leq \|S\|_2 \|M\|_2 \leq \frac{2\|\Delta_p\|_2}{\sigma_{\min}(D_{(A,B)}^p) - \|\Delta_p\|_2} \left\| \begin{pmatrix} A \\ B \end{pmatrix} \right\|_2. \quad (\text{B.48})$$

Combining (B.48) with (B.33), we obtain a final bound

$$\begin{aligned} \|\widetilde{A}_p - \mathring{A}_p\|_2 &\leq \|\widetilde{A}_p - A_p\|_2 + \|A_p - \mathring{A}_p\|_2 \\ &\leq \left[(1 + 2\tau)^{2p} + (1 + \tau)^p - 2 + \frac{2\|\Delta_p\|_2}{\sigma_{\min}(D_{(A,B)}^p) - \|\Delta_p\|_2} \right] \left\| \begin{pmatrix} A \\ B \end{pmatrix} \right\|_2, \end{aligned} \quad (\text{B.49})$$

which also applies to $\|\widetilde{B}_p - \mathring{B}_p\|_2$.

Step Eight: Bound τ by enforcing $\|\tilde{A}_p - \mathring{A}_p\|_2, \|\tilde{B}_p - \mathring{B}_p\|_2 \leq \delta \|(A/B)\|_2$.

Given (B.49), we obtain the desired bound on $\|\tilde{A}_p - \mathring{A}_p\|_2$ and $\|\tilde{B}_p - \mathring{B}_p\|_2$ provided each of $(1 + 2\tau)^{2p} - 1$, $(1 + \tau)^p - 1$, and $\frac{2\|\Delta_p\|_2}{\sigma_{\min}(D_{(A,B)}^p) - \|\Delta_p\|_2}$ is at most $\frac{\delta}{3}$. We focus on the latter, since it is the largest. Here, we note that taking $\|\Delta_p\|_2 \leq \frac{\delta}{9}\sigma_{\min}(D_{(A,B)}^p)$ guarantees not only that the bound (B.46) holds but also

$$\frac{2\|\Delta_p\|_2}{\sigma_{\min}(D_{(A,B)}^p) - \|\Delta_p\|_2} \leq \frac{2\delta}{9 - \delta} < \frac{\delta}{3}, \quad (\text{B.50})$$

as desired. Appealing to (B.43) and Definition 2.3, we obtain $\|\Delta_p\|_2 \leq \frac{\delta}{9}\sigma_{\min}(D_{(A,B)}^p)$ by requiring that each of $14\tau(1 + \tau)^{p-1}$, $(p-1)[(1 + 15\tau)(1 + 2\tau)^{2p} - (1 + \tau)^p]$, and $(1 + \tau)^p - 1$ is bounded by $\frac{\delta}{54\kappa_{\text{IRS}}(A, B, p)}$. Once again, we focus on the largest of these terms, which in this case is $X = (p-1)[(1 + 15\tau)(1 + 2\tau)^{2p} - (1 + \tau)^p]$, assuming $p > 1$.

We begin by rewriting X as follows:

$$X = (p-1)(1 + 2\tau)^{2p} \left[1 + 15\tau - \left[1 - \tau \left(\frac{3 + 4\tau}{(1 + 2\tau)^2} \right) \right]^p \right]. \quad (\text{B.51})$$

Since $\tau \left(\frac{3 + 4\tau}{(1 + 2\tau)^2} \right) \leq 1$, we can bound X from above via Bernoulli's inequality

$$\begin{aligned} X &\leq (p-1)(1 + 2\tau)^{2p} \left[1 + 15\tau - \left[1 - p\tau \left(\frac{3 + 4\tau}{(1 + 2\tau)^2} \right) \right] \right] \\ &= (p-1)(1 + 2\tau)^{2p} \tau \left[15 + p \left(\frac{3 + 4\tau}{(1 + 2\tau)^2} \right) \right] \\ &\leq 3\tau(p-1)(p+5)(1 + 2\tau)^{2p}, \end{aligned} \quad (\text{B.52})$$

where the last inequality follows by loosely bounding $\frac{3 + 4\tau}{(1 + 2\tau)^2} \leq 3$. Finally assuming $(1 + 2\tau)^{2p} \leq 2$, we obtain a final bound

$$X \leq 6\tau(p-1)(p+5) = 6\tau(p^2 + 4p - 5), \quad (\text{B.53})$$

which implies a criterion on τ :

$$\tau \leq \frac{\delta}{324\kappa_{\text{IRS}}(A, B, p)(p^2 + 4p - 5)}. \quad (\text{B.54})$$

Note that if $p = 1$, and therefore $X = 0$, we require instead $15\tau \leq \frac{\delta}{18\kappa_{\text{IRS}}(A, B, p)}$ above, which is clearly satisfied by (B.54). It is similarly not hard to show that this requirement on τ guarantees the remaining bounds and therefore yields $\|\tilde{A}_p - \mathring{A}_p\|_2, \|\tilde{B}_p - \mathring{B}_p\|_2 \leq \delta \|(A/B)\|_2$.

It remains to show that \mathring{A}_p and \mathring{B}_p can be obtained via exact-arithmetic repeated squaring. This follows from Lemma B.4; exact-arithmetic repeated squaring implies an alternative block-QR factorization of $M\Pi$, which is equivalent to (B.47) up to a rotation/reflection. Since such a rotation/reflection can be baked into the final QR factorization computed by exact-arithmetic repeated squaring (which is agnostic to the specific QR factorizations used), \mathring{A}_p and \mathring{B}_p are indeed exact outputs of repeated squaring satisfying $\mathring{A}_p^{-1}\mathring{B}_p = (A^{-1}B)^{2p}$.

C Additional Numerical Examples

This appendix contains additional numerical tests. Here, we consider a modified version of the setup used in Section 4. We again construct a 500×500 diagonal matrix Λ according to (4.2), though this time we allow Λ_+ and Λ_- to sample from all of the right/left half planes, respectively, instead of restricting to the real line. Drawing a Haar unitary eigenvector matrix $V \in \mathbb{C}^{500 \times 500}$ and letting B be a random complex Gaussian matrix, we then set

$$A = BV\Lambda V^H. \quad (\text{C.1})$$

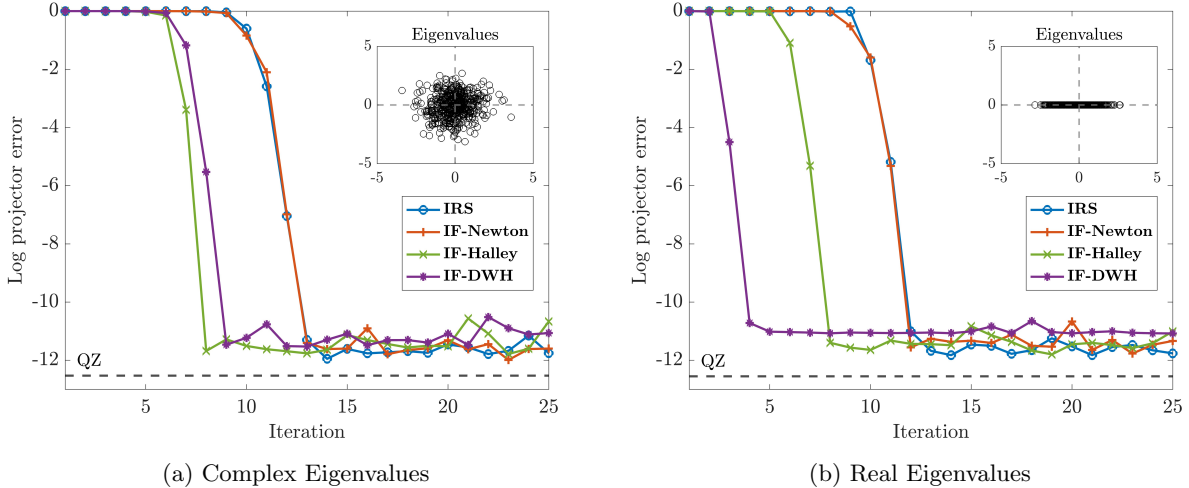


Figure 5: Forward approximation error for computing a spectral projector of a 500×500 pencil (A, B) constructed according to (C.1). We consider two cases, where the eigenvalues of (A, B) are either real or complex. In each case, we plot the eigenvalues of (A, B) and mark the error produced by QZ – which approximates the projector by computing first a full eigendecomposition and then a QR factorization of corresponding eigenvectors – as a benchmark.

In this case, $B^{-1}A = V\Lambda V^H$ is Hermitian and a spectral projector corresponding to eigenvalues in the right half plane can be obtained from the leading columns of V .

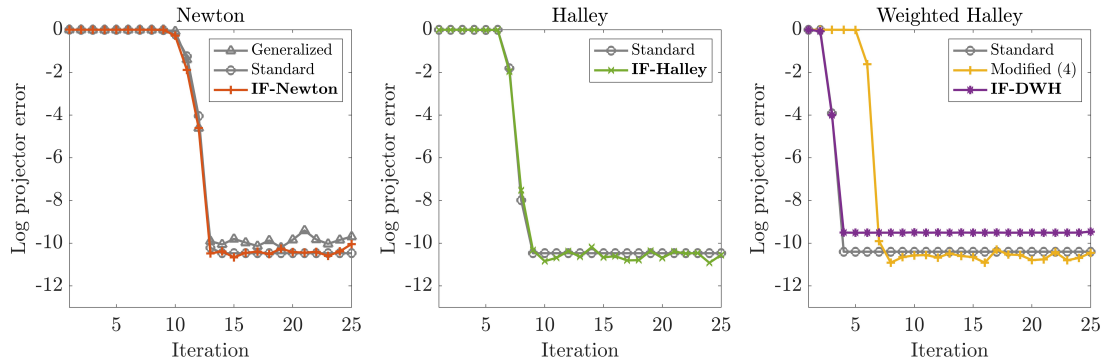
Figure 5 uses this construction to test **IRS**, **IF-Newton**, **IF-Halley**, and **IF-DWH** on problems with complex eigenvalues, repeating the plot of Figure 3 for two choices of Λ . The only difference between the resulting plots is the number of iterations required for **IF-DWH** to converge, an empirical reminder that the dynamic weighting scheme is only relevant for problems with real eigenvalues.

As a final test, we verify the benefits of working inverse-free. To that end, we again return to real eigenvalues and compare each of **IF-Newton**, **IF-Halley**, **IF-DWH** and the modified Halley iteration to alternative “standard” implementations, which explicitly form $B^{-1}A$ and apply the corresponding single-matrix iteration, with inversion. For **IF-Newton**, we also compare against the original generalized Newton iteration of Gardiner and Laub [21], which uses inversion but avoids forming $B^{-1}A$. **IRS** is omitted here since an algorithm based on explicit squaring performs poorly on even well-conditioned problems.

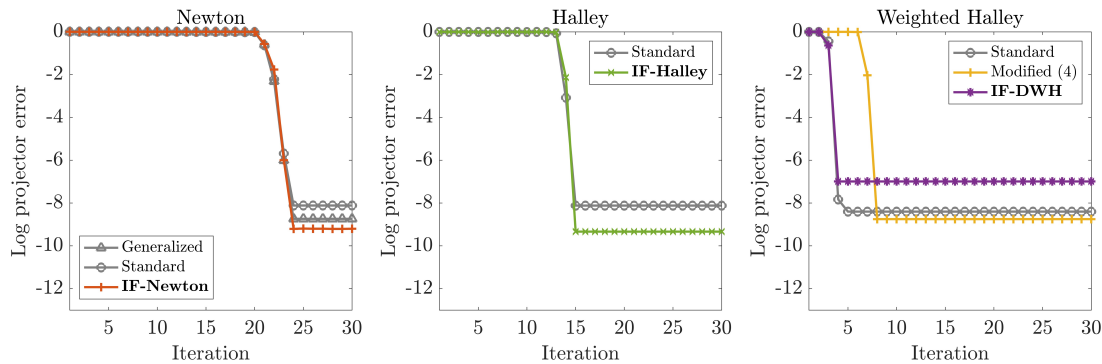
We present this comparison in two settings: one in which the eigenvalues are sampled from $\pm|\mathcal{N}(0, 1)|$ (e.g., the poorly-separated case from Section 4) and one in which the eigenvalues are sampled in the same way but two are replaced by $\pm 10^{-6}$. Since the condition number of $B^{-1}A$ is clearly the ratio of the largest and smallest eigenvalues (in magnitude) of (A, B) , this ensures that in the first case $B^{-1}A$ is relatively well-conditioned while in the latter it is relatively poorly-conditioned.

Tracking forward projector error for each method with and without inversion yields Figure 6. We see here that the inverse-free iterations, with the exception of **IF-DWH**, are essentially equivalent to their alternatives when $B^{-1}A$ is well-conditioned but significantly more accurate when it is not. Note here that B is well-conditioned with high probability, meaning error incurred when forming $B^{-1}A$ is unlikely to explain the gap in performance alone. This is also to say nothing of more contrived examples in which the standard iterations are guaranteed to perform poorly – e.g., the standard Halley iteration on a problem with an eigenvalue near $\frac{i}{\sqrt{3}}$.

Interestingly, the dynamically weighted Halley iteration appears to avoid the stagnation problem observed in Section 4 when implemented with inversion. This lends further support to the idea that the instability is inherent to our QR-based implementation.



(a) Well-conditioned: eigenvalues drawn randomly from $\pm\mathcal{N}(0, 1)$; $\kappa_2(B^{-1}A) = 1.73 \times 10^3$.



(b) Poorly-conditioned: eigenvalues are the same as in (a) with two replaced by $\pm 10^{-6}$; $\kappa_2(B^{-1}A) = 3.20 \times 10^6$.

Figure 6: Performance of various sign-function-based iterations with and without inversion. For each iteration type, “Standard” refers to an implementation that explicitly forms $B^{-1}A$ and applies a single-matrix version of the iteration (that requires inversion). For Newton, “Generalized” refers to the algorithm of Gardiner and Laub [21]. In each case we again compute a spectral projector of a 500×500 pencil (A, B) constructed according to (C.1), where the choice of eigenvalues determines the conditioning of $B^{-1}A$. Projector error is the same as in the previous figures.